

UNCLASSIFIED

AD NUMBER

ADB080654

LIMITATION CHANGES

TO:

Approved for public release; distribution is unlimited.

FROM:

Distribution authorized to U.S. Gov't. agencies only; Test and Evaluation; FEB 1984. Other requests shall be referred to Chemical Research and Development Center, Attn: DRSMC-CLB-PS, Aberdeen Proving Ground, MD 21010.

AUTHORITY

USAMCCOM ltr, 6 nov 1984

THIS PAGE IS UNCLASSIFIED



Improved Methods to Invert the Particle Size Distribution Function from Mie Scattering Measurements

B. P. Curry and E. L. Kiech
Calspan Field Services, Inc.

Property of U. S. Air Force
AEDC LIBRARY
F40600-81-C-0004

February 1984

**TECHNICAL REPORTS
FILE COPY**

Final Report for Period October 1982 – September 1983

Distribution limited to U.S. Government agencies only; this document contains information on test and evaluation of military hardware; February 1984. Other requests for this document must be referred to Commander, USAMCCOM, Chemical Research and Development Center, ATTN: DRSMC-CLB-PS, Aberdeen Proving Ground, MD 21010.

INFORMATION SUBJECT TO EXPORT CONTROL LAWS

This document may contain information subject to the International Traffic in Arms Regulation (ITAR) or the Export Administration Regulation (EAR) of 1979 which may not be exported, released or disclosed to foreign nationals inside or outside the United States without first obtaining an export license. A violation of the ITAR or EAR may be subject to a penalty of up to 10 years imprisonment and a fine of \$100,000 under 22 U.S.C. 2778 or Section 2410 of the Export Administration Act of 1979. Include this notice with any reproduced portion of this document.

**ARNOLD ENGINEERING DEVELOPMENT CENTER
ARNOLD AIR FORCE STATION, TENNESSEE
AIR FORCE SYSTEMS COMMAND
UNITED STATES AIR FORCE**

NOTICES

When U. S. Government drawings, specifications, or other data are used for any purpose other than a definitely related Government procurement operation, the Government thereby incurs no responsibility nor any obligation whatsoever, and the fact that the government may have formulated, furnished, or in any way supplied the said drawings, specifications, or other data, is not to be regarded by implication or otherwise, or in any manner licensing the holder or any other person or corporation, or conveying any rights or permission to manufacture, use, or sell any patented invention that may in any way be related thereto.

Qualified users may obtain copies of this report from the Defense Technical Information Center.

References to named commercial products in this report are not to be considered in any sense as an endorsement of the product by the United States Air Force or the Government.

APPROVAL STATEMENT

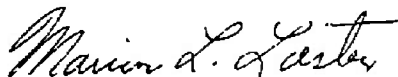
This report has been reviewed and approved.



KENNETH H. LENERS, Captain, USAF
Directorate of Technology
Deputy for Operations

Approved for publication:

FOR THE COMMANDER



MARION L. LASTER
Director of Technology
Deputy for Operations

UNCLASSIFIED

SECURITY CLASSIFICATION OF THIS PAGE (When Data Entered)

REPORT DOCUMENTATION PAGE		READ INSTRUCTIONS BEFORE COMPLETING FORM
1. REPORT NUMBER AEDC-TR-83-52	2. GOVT ACCESSION NO.	3. RECIPIENT'S CATALOG NUMBER
4. TITLE (and Subtitle) IMPROVED METHODS TO INVERT THE PARTICLE SIZE DISTRIBUTION FUNCTION FROM MIE SCATTERING MEASUREMENTS		5. TYPE OF REPORT & PERIOD COVERED Final Report, Oct. 1, 1982 - Sept. 30, 1983
		6. PERFORMING ORG REPORT NUMBER
7. AUTHOR(s) B. P. Curry and E. L. Kiech, Calspan Field Services, Inc.		8. CONTRACT OR GRANT NUMBER(s)
9. PERFORMING ORGANIZATION NAME AND ADDRESS Arnold Engineering Development Center/DOT Air Force Systems Command Arnold Air Force Station, TN 37389		10. PROGRAM ELEMENT, PROJECT, TASK AREA & WORK UNIT NUMBERS Program Element 921C18
11. CONTROLLING OFFICE NAME AND ADDRESS Commander, USAMCCOM Chemical Research and Development Center ATTN: DRSMC-CLB-PS Aberdeen Proving Ground, MD 21010		12. REPORT DATE February 1984
		13. NUMBER OF PAGES 45
14. MONITORING AGENCY NAME & ADDRESS (if different from Controlling Office)		15. SECURITY CLASS (of this report) UNCLASSIFIED
		15a. DECLASSIFICATION/DOWNGRADING SCHEDULE N/A
16. DISTRIBUTION STATEMENT (of this Report) Distribution limited to U.S. Government agencies only; this report contains information on test and evaluation of military hardware; February 1984; other requests for this document must be referred to Commander, USAMCCOM, Chemical Research and Development Center, ATTN: DRSMC-CLB-PS, Aberdeen Proving Ground, MD 21010.		
17. DISTRIBUTION STATEMENT (of the abstract entered in Block 20, if different from Report)		
18. SUPPLEMENTARY NOTES Available in Defense Technical Information Center (DTIC).		
19. KEY WORDS (Continue on reverse side if necessary and identify by block number) particle size aerosols Mie scattering inversion regression analysis		
20. ABSTRACT (Continue on reverse side if necessary and identify by block number) Two previously reported methods to invert the particle size dis- tribution function (PSDF) from Mie scattering measurements on aerosol clouds are reconsidered and improvements are made in both. One of these methods - nonlinear regression - is described in greater detail than has previously been reported. Both techniques are tested by inverting the PSDF from noisy, synthetic scattering		

UNCLASSIFIED

SECURITY CLASSIFICATION OF THIS PAGE(When Data Entered)

20. ABSTRACT (Continued)

data. Some situations which result in ambiguities in determining the PSDF are identified and analyzed with the aid of residual error contour plots.

UNCLASSIFIED

SECURITY CLASSIFICATION OF THIS PAGE(When Data Entered)

PREFACE

The work reported herein was performed by the Arnold Engineering Development Center (AEDC), Air Force Systems Command (AFSC) for the Chemical Research and Development Center (CRDC), U. S. Army Armament, Munitions, and Chemical Command (AMCCOM), Aberdeen Proving Ground, Maryland. These results were obtained by Calspan Field Services, Inc., AEDC Division, operating contractor for the aerospace flight dynamics testing at AEDC, AFSC, Arnold Air Force Station, Tennessee, Under Project No. D244PW. The CRDC Project Monitor was Dr. Jerold Bottiger; Capt. K. Leners was the AEDC Project Manager. The data analysis was completed on August 31, 1983, and the manuscript was submitted for publication on September 30, 1983.

CONTENTS

1.0 INTRODUCTION	5
2.0 LIGHT SCATTERING BACKGROUND	5
2.1 Solution of Integral Scattering Equation	7
2.2 Constrained Eigenfunction Expansion	7
2.3 Nonlinear Regression	11
2.4 Residual Error Contour Analysis	13
3.0 INVERSION OF THE PSDF FROM NOISY, SYNTHETIC MIE SCATTERING DATA	14
4.0 CONCLUDING REMARKS	16
REFERENCES	18

ILLUSTRATIONS

1. Number Normalized Particle Size Distribution Function Used to Generate the Scattering Input Spectrum of Fig. 2	19
2. Computed Backscattering Spectrum for n-Butanol Droplets Having the PSDF Shown in Fig. 1	20
3. Residual Error Contours for Recovery of the PSDF of Fig. 2 from the Scattering Inputs of Fig. 1—No Additional Noise	21
4. Residual Error Contours for Recovery of the PSDF of Fig. 2 from the Scattering Inputs of Fig. 1 with 6.7-percent Gaussian Noise Level	22
5. Number Normalized PSDF Recovered from the Scattering Inputs of Fig. 1 with 6.7-percent Gaussian Noise Level	23
6. Mass Normalized PSDF Recovered from the Scattering Inputs of Fig. 1 with 6.7-percent Gaussian Noise Level	24
7. Number Normalized PSDF Used to Generate the Scattering Inputs in Table 2	25
8. Number Normalized PSDF Recovered from the Scattering Inputs of Table 2 with 3-percent Gaussian Noise Level	26
9. Residual Error Contours for Recovery of the PSDF of Fig. 7 from the Scattering Inputs Listed in Table 2	27
10. Mass Normalized PSDF Recovered from the Scattering Inputs of Table 2 with 3-percent Gaussian Noise Level	28
11. Number Normalized “Zero Centered” PSDF Used to Generate the Scattering Inputs in Table 3	29
12. Number Normalized PSDF Recovered from the Scattering Inputs of Table 3 with 3-percent Gaussian Noise Level	30

<u>Figure</u>	<u>Page</u>
13. Residual Error Contours for Recovery of the PSDF of Fig. 11 from the Scattering Inputs Listed in Table 3	31
14. Mass Normalized PSDF Recovered from the Scattering Inputs of Table 3 with 3-percent Gaussian Noise Level	32
15. Number Normalized Bimodal PSDF Used to Generate the Scattering Inputs in Table 4	33
16. Number Normalized PSDF Recovered from the Scattering Inputs of Table 4 with 3-percent Gaussian Noise Level	34
17. Residual Error Contours for Recovery of the PSDF of Fig. 15 from the Scattering Inputs Listed in Table 4	35
18. Mass Normalized PSDF Recovered from the Scattering Inputs of Table 4 with 3-percent Gaussian Noise Level	36
19. Number Normalized Bimodal PSDF Regressed from the Scattering Inputs of Table 5 with 5-percent Gaussian Noise Level	37
20. Mass Normalized Bimodal PSDF Regressed from the Scattering Inputs of Table 5 with 5-percent Gaussian Noise Level	38
21. Number Normalized Bimodal PSDF Deconvolved from the Scattering Inputs of Table 5 with 5-percent Gaussian Noise Level	39
22. Mass Normalized Bimodal PSDF Deconvolved from the Scattering Inputs of Table 5 with 5-percent Gaussian Noise Level	40

TABLES

1. Refractive Indices used to Generate the Scattering Inputs Listed in Tables 2 - 4	41
2. Error-Free Scattering Inputs for the PSDF in Figure 7	41
3. Error-Free Scattering Inputs for the PSDF in Figure 11	42
4. Error-Free Scattering Inputs for the PSDF in Figure 15	42
5. Error-Free Scattering Inputs for the PSDF in Figure 19	43
 NOMENCLATURE	 44

1.0 INTRODUCTION

Since 1981, the U. S. Army Chemical Research and Development Center (USAMCCOM) has sponsored research at AEDC to develop and test methods to invert the particle size distribution function (PSDF) from Mie scattering measurements on homogeneous, spherical particle, aerosol clouds. The two most successful inversion techniques developed during this effort were reported in Ref. 1. The present report describes improvements made in the inversion techniques during the current contract period. In addition, this report presents a more detailed description of one of the inversion techniques (nonlinear regression) than has been previously presented. Further, a graphical procedure to determine the size range over which the PSDF should be inverted and to localize the modes of the PSDF is demonstrated. Finally, examples of PSDF's recovered from noisy, synthetic Mie scattering data are presented to demonstrate the utility of these techniques for the development of practical particle diagnostics methods.

2.0 LIGHT SCATTERING BACKGROUND

The formalism by which light scattering measurements are related to calculable Mie scattering functions has been presented in Refs. 1 and 2. Here, it suffices to state the Fredholm integral equation which describes Mie scattering from a polydisperse distribution of uniform dielectric spheres.

$$G(Y_i) + E(Y_i) = \frac{1}{N} \int_0^{\infty} K(X, y_i) f(X) dX \quad (1)$$

$$\text{where } N_0 = \int_0^{\infty} K_0(X) F(x) dX$$

In this equation the solution variable X denotes either particle diameter or size parameter ($X = \pi D/\lambda$), and the functional parameter $G(y)$ denotes a suitably normalized measurement or combination of measurements of the scattered light intensity as a function of the scattering angle, wavelength, and state of polarization of the light scattered by a localized distribution of particles, whose number normalized PSDF is $f(X)$. The set of independent measurement variables (y_i), $i = 1, 2, \dots, N$ is finite and discrete, even though the PSDF is regarded as a continuous function of X . A more complete representation of Eq. (1), allowing for the notation associated with each of the three types of independent scattering variable is stated in Ref. 2, and all the PSDF inversion codes developed in this project conform to the variable ordering convention stated therein.

Equation (1) is an example of what has been called the "ill-posed problem," both because of the pathological behavior of the Mie scattering kernels (differential scattering

cross sections, in the present context) and because of the presence of the residual errors $E(y_i)$. These are an inextricable combination of experimental and computationally induced errors. All successful solution procedures of which we are aware depend on the use of some kind of scheme to minimize a weighted sum of the squares of the residual errors. The constrained eigenfunction expansion procedure, which we reported in Ref. 1, uses formal variational methods to obtain that solution of Eq. (1) which minimizes the squared residual errors (inversely weighted by the estimated standard deviations for each input channel) subject to specified constraints. The nonlinear regression procedure introduced in Ref. 1 and on which we elaborate further involves no explicit constraints, but implicitly incorporates constraints through the use of fitting functions of predetermined form.

Except for the normalizing factor N_0 , Eq. (1) has been discussed extensively in previous work (Refs. 1 and 2). If N_0 is regarded as a normalization constant, it can simply be absorbed into the definition of the scattering kernels, and the previous treatment of Eq. (1) and associated solution methods will then stand unamended. Two of the four solution techniques developed during the course of this project were originally predicated on the assumption that the normalization kernel $K_0(X)$ could be chosen in such a fashion as to minimize the dependence of the normalization factor N_0 on the PSDF, thus permitting N_0 to be regarded as a constant. Both the nonlinear (modified Towmey-Chahine) inversion method presented in Ref. 2 and the nonlinear regression procedure of Ref. 1 allow N_0 to be evaluated numerically at intermediate steps during the iteration cycles on which these solution techniques are based; consequently, N_0 is regarded, correctly, as a function of the PSDF in both these procedures. One of the accomplishments reported herein is the generalization of the constrained eigenfunction expansion method presented in Ref. 1 to allow retention of the functional dependence of N_0 on the parameters which characterize the PSDF. Clearly, adoption of this point of view requires that one must abandon the notion that the PSDF inversion problem is linear, if one uses ratios of scattering measurements instead of absolute measurements.

What is gained, as a consequence of this acceptance of the inherent nonlinearity of the problem, is the assurance that the recovered PSDF is more accurate than the results obtained with N_0 treated as a constant and, equally important, that the residual error associated with the recovered PSDF can be considered a fairly good approximation to the (unknown) actual experimental error in the scattering inputs. Retention of the functional dependence of N_0 on the PSDF parameters has been a characteristic of our nonlinear regression algorithm since its origin; however, our constrained eigenfunction deconvolution procedure has only recently been generalized to incorporate this feature.

2.1 SOLUTION OF THE INTEGRAL SCATTERING EQUATION

To solve Eq. (1), which is a Fredholm integral equation of the first kind if N_0 is temporarily regarded as a constant, let us consider parametric forms of the PSDF

$$f_1(X) = f_1(X, C_1, C_2, \dots, C_N) \quad (2)$$

and

$$f_2(X) = f_2(X, C_1, C_2, \dots, C_r, P_1, P_2, \dots, P_s) \quad (3)$$

where N is the total number of measurements and $r + s \leq N$

In Eqs. (2) and (3) the constants C_1, C_2, \dots , are to be regarded as members of a set of linear expansion coefficients for the expansion of the PSDF in basis functions. Our first procedure considers the basis functions to be known functions of X , having no additional parameters. The linear expansion coefficients are determined by a formal variational procedure in which the sum of the squared residual errors is minimized subject to a specified constraint. This solution procedure was designated a "constrained eigenfunction expansion" in Ref. 1 because the basis functions are eigenfunctions of the Mie scattering kernels.

Our second solution procedure involves a linear expansion of the PSDF in basis functions which depend in a nonlinear fashion on X and on the parameters P_1, P_2, \dots, P_s . The composite set of parameters $\{C_1, C_2, \dots, C_r\} + \{P_1, P_2, \dots, P_s\}$ is regarded as the set of regression parameters for a multivariate, nonlinear regression procedure which seeks to minimize the sum of the squared residual errors. We have used as basis functions lognormal distributions, cubic splines, Gaussians, and other functions whose height and width are taken to be parameters of the regression.

In the next two sections we discuss the most significant characteristics of both these PSDF inversion procedures. Since the constrained eigenfunction expansion solution was derived in considerable detail in Ref. 1, we review in Section 2.2 only the most significant results of that derivation. The nonlinear regression technique is, however, discussed in considerable detail in Section 2.3.

2.2 CONSTRAINED EIGENFUNCTION EXPANSION

By a well known theorem, one can show that the optimum complete basis set for a linear expansion of the PSDF consists of eigenfunctions of the symmetric kernel operator

$$M_{(X',X)} = \sum_{i=1}^N K(X',y_i) K(X,y_i)$$

These eigenfunctions can be computed from eigenvectors of the kernel covariance matrix (in the input domain), which is defined as

$$N(y_i,y_j) = \int_0^{\infty} K(X,y_i) K(X,y_j) dX \quad (4)$$

by use of the normalized transformation

$$\phi_i(X) = \lambda_i^{-1/2} \sum_{k=1}^N U_i(y_k) K(X,y_k) \quad (5)$$

where U_i and λ_i are, respectively, the "ith" eigenvector and the "ith" eigenvalue of the kernel covariance matrix N . The direct solution of Eq. (4) which minimizes the residual errors without introducing any solution constraints was published by Capps, et al. (Ref. 3). Recently, we generalized this solution to incorporate variational constraints and inverse weighting of the kernels by the estimated imprecision values (square root of the estimated variances) for each input channel (Ref. 1). Our derivation shows that the solution expansion coefficients which incorporate a trial function constraint can be written as

$$C_i = \frac{\frac{\gamma}{\lambda_i} (C_i^T + C_i^0)}{\left(1 + \frac{\gamma}{\lambda_i}\right)} \quad (6)$$

where the coefficients $C_i^T = \int F_i^T(X) \phi_i(X) dX$ are the expansion coefficients for the trial function $f^T(X)$ and the coefficients C_i^0 are the imprecision weighted direct solution coefficients

$$C_i^0 = \lambda_i^{1/2} \sum_{k=1}^N U_i(y_k) \frac{G(y_k)}{\Delta G(y_k)} \quad (7)$$

In these equations $\Delta G(y_k)$ designates the estimated imprecision of the "kth" scattering measurement and the eigenfunctions, eigenvectors, and eigenvalues are calculated as previously indicated, but are based on the imprecision weighted kernels $K^w(X,y_i) = K(X,y_i)/\Delta G(y_i)$. In addition, the normalization function $N_0 = \int_0^{\infty} K_0(X)f(X)dX$ has, for the moment, been absorbed into the kernels as a normalization constant, restricting the

choice of the normalization kernel $K_o(X)$ to being slowly a varying function of X . This restriction will later be removed. The PSDF is expanded in terms of those coefficients as

$$f(X) = \sum_i C_i \phi_i(X) \quad (8)$$

and the residual errors are calculated from

$$E(y_i) = \frac{\sum_j C_j \lambda_j^{1/2} U_j(y_i) - G(y_i)}{\Delta G(y_i)} \quad (9)$$

If one denotes the error-free PSDF by $f^o(x)$, then the solution error norm is bounded by

$$\int_0^\infty |f(X) - f^o(X)|^2 dX \leq \sum_{i=1}^N \lambda_i^{-1} \sum_{k=1}^N \left| \frac{E(y_k)}{\Delta G(y_k)} \right|^2 \quad (10)$$

showing that the only solution components which contribute valid information to the recovered PSDF are those which satisfy

$$\lambda_i > > \sum_{k=1}^N \left| \frac{E(y_k)}{\Delta G(y_k)} \right|^2 \quad (11)$$

as was first shown by Twomey (Ref. 4). Invalid solution components must be suppressed, else the recovered PSDF will exhibit unphysical behavior. Suppression can be accomplished by deleting from the PSDF expansion those components which violate the above inequality (as was done in Ref. 3) or, by use of the constrained expansion coefficients presented here and in Ref. 1, or by a combination of the two methods.

If one knew the actual errors in each measurement channel, the residual errors resulting from both smoothing and experimental errors could be computed from

$$\frac{E(y_i)}{\Delta G(y_i)} = \sum_{j=1}^N \frac{U_j(y_i)}{(1 + \frac{\gamma}{\lambda_i})} \left[\frac{\gamma}{\lambda_i^{1/2}} (C_j^T - C_j^o) + \sum_{k=1}^N U_j(y_k) \frac{\delta G(y_k)}{\Delta G(y_k)} \right] \quad (12)$$

where $\delta G(y_k)$ denotes the (unknown) actual error in the "kth" measurement. This equation shows that, as γ increases, the effect of actual experimental error is damped at the expense of the introduction of error caused by smoothing. In actuality, since one doesn't know the actual experimental errors, the residual errors must be regarded as being entirely the result of

the smoothing process. If one can reliably estimate the optimum value of the smoothing parameter, the computed residual error will approximately equal the experimental error.

Our solution procedure determines the optimum smoothing level by seeking a minimum in a parameter which is denoted the "Residual Relative Variance" (RRV) in Ref. 1. This parameter is a weighted average of the residual errors. Its minima are found to correspond to the values of γ at which near equality is found between one or more pairs of the coefficients C_i and $\gamma/\lambda(C_i^2)$. In practice, our solution technique employs a doubly iterative calculation sequence in which, at any stage of iteration, the smoothing parameter is increased until either a true minimum of the RRV is found (with respect to γ) or else the slope of the RRV is found to be negative and flat within a specified tolerance. The solution is then checked to see whether it differs from the previous iterate, within a specified tolerance. If the difference exceeds the tolerance, the current solution is taken to be the trial function for the next iteration cycle. The entire iteration sequence is begun by the specification of the initial trial function, and the sensitivity of the results to the choice of initial trial function is controlled by the specification of the "flat slope" criterion and the iteration convergence criterion.

Once the PSDF has been determined, solution error bounds can be calculated, based on the assumption that the input errors are Gaussian. If the solution is based on the use of imprecision weighted kernels, the PSDF variance is rigorously expressed as

$$|\Delta f(X)|^2 = \sum_{i=1}^N \lambda_i^{-1} \frac{|\phi_i(X)|^2}{1 + \frac{\gamma}{\lambda_i}} \quad (13)$$

If the solution is based on unweighted kernels, the PSDF variance can be calculated, approximately, from

$$|\Delta f(X)|^2 = \sum_{i=1}^N \lambda_i^{-1} |\phi_i'(X)|^2 \frac{\sum_{k=1}^N |U_i'(Y_k) \Delta G(Y_k)|^2}{1 + \frac{\gamma}{\lambda_i} \sum_{k=1}^N |U_i'(y_k) \Delta G(y_k)|^2} \quad (14)$$

where the prime denotes eigenfunctions, eigenvectors, or eigenvalues of the unweighted scattering kernels.

The equations presented in this section and in Ref. 1 reduce identically to those of Ref. 3 when $\gamma \rightarrow 0$ and $\Delta G(y_i) \rightarrow 1$. If the imprecision of each measurement is proportional to the magnitude of each measurement, weighting by input imprecision values is equivalent to

weighting by the kernel norms, as was done in Ref. 3. In such a case, Eqs. (13) and (14) are also equivalent.

The preceding equations were all derived under the assumption that the normalization kernel $K_0(X)$ varied sufficiently slowly to permit the normalization function $N_0 = \int_0^\infty K_0(X) dX$ to be treated as a constant. This restriction is easily removed if the normalizing kernel is representable as a member of or a linear combination of members of the set of kernels which correspond to the input channels. Thus, if

$$K_0(X) = \sum_{i=1}^N a_i K(X, y_i) \quad (15)$$

where the a_i are arbitrary expansion coefficients, the normalization function can be evaluated, approximately, as

$$N_0 = \sum_{i=1}^N a_i \Delta G(y_i) \sum_{j=1}^N C_j^T \lambda_j^{1/2} U_j(y_i) \quad (16)$$

since the trial coefficients are the PSDF expansion coefficients for the previous iteration cycle. When this form of the normalization function is used, the PSDF expansion coefficients must be modified in Eq. (6) by replacing each direct solution coefficient C_i by the product $N_0 C_i$. Similarly, the smoothed expansion coefficients C_j in Eq. (9) must be replaced by the ratio C_j/N_0 to calculate the residual errors correctly. We refer to the use of N_0 as a functional dependent on the properties of the PSDF in the solution procedure as "active normalization," whereas "passive normalization" indicates the consideration of N_0 as a constant which can be absorbed into the definition of the kernels. The solution procedure is sometimes less rapidly convergent when active normalization is employed, but it is more stable in the presence of experimental errors than when passive normalization is used. Further, the residual error corresponding to convergence of the iteration sequence has been found to be a fairly good estimate of the experimental error in the inputs when deconvolutions of simulated scattering data containing known levels of Gaussian-distributed noise have been performed.

2.2 NONLINEAR REGRESSION

Our second inversion procedure was originally developed for the Naval Air Test Center, Trenton, New Jersey. This technique has been extensively modified for application to the particle diagnostics needs of CRDC and the AEDC. This inversion procedure seeks to determine the PSDF by a nonlinear regression involving numerical application of the principle of least squares.

Assuming that $f(X)$ can be adequately expressed as a function of the parameters (P_i) and that the errors, $E(y_i)$, in Eq. (I) are normally distributed, the principle of least squares states that the best approximation to $f(X)$ is that function $f(X, \{P_i\})$ in which the choice of the set of regression parameters $\{P_i\}$ minimizes the sum of the squares of the residuals between the calculated and measured scattering inputs $G(y_i)$, weighted by the inverse of each input's associated standard deviation. The selection of the fitting function, $f(X, \{P_i\})$ is a fundamental part of the regression procedure and is based on several considerations. If $f(X)$ is known to be of a certain type (such as a lognormal), then the fitting function should be of the same type. Usually, however, nothing is known beforehand about the characteristics of $f(X)$. In this case a wide range of fitting functions can be selected and the regression technique should specify the best set of parameters, given the functional form of the fitting function and the measured inputs $G(Y_i)$. Since each independent parameter lends the fit an additional degree of freedom, the maximum number of parameters should be used for the most flexible fitting function, subject to limits which will now be stated.

Three major factors limit the number of usable, independent regression parameters:

1. The number of independent parameters must be no more than the number of independent inputs $G(y_i)$.
2. As the fitting function becomes more flexible, more of the noise in the inputs will be incorrectly interpreted as good data. A judgment must be made (based on the signal-to-noise ratio of the data) regarding how much flexibility the fitting function can have and still remain acceptably free of the influence of noise.
3. Computer limits restrict one's flexibility in finding a minimum in the surface representing the residual errors as a function of the regression parameters. As more parameters are added, the time required to find a minimum in the residual error hypersurface increases rapidly, and the hypersurface tends to develop secondary minima, sometimes causing the nonlinear regression algorithm to converge to a local minimum instead of the absolute minimum of the residual error hypersurface.

Before development of the current procedure, several standard nonlinear regression algorithms were used to determine $f(X, \{P_i\})$ for various case studies of synthetic data. During these studies, it became apparent that the heavy coupling among the parameters of $f(X, \{P_i\})$ made convergence very difficult for the standard iterative procedures. Consequently, a new nonlinear regression procedure was developed which was expected to be more stable when dealing with highly coupled parameters. The procedure starts with

initial values for the parameters of $f(X, \{P_i\})$, yielding an initial value for Q , the sum of the squared residual errors. Each succeeding step of the iteration seeks the minimum of Q with respect to a multiplet of parameters of increasing order. For each multiplet, the minimum is sought repeatedly with respect to each member of the multiplet (with all other members held constant) until no further reduction in Q is found. The program then repeats this process with the next higher order multiplet until the order of the last convergent multiplet equals the number of parameters. The procedure used to minimize Q with respect to each parameter is quadratic minimization. Three Q 's are calculated corresponding to three initial values of a parameter. The vertex of the parabola through these three points is used as the next estimate of the minimum and replaces one of the three initial points. The process continues until there is no further reduction in Q . Since this nonlinear regression technique seeks the minimum closest to the starting point, the regression must be started with several different sets of initial parameters to determine whether there are any other minima in the Q hypersurface within the region of interest.

2.3 RESIDUAL ERROR CONTOUR ANALYSIS

The choice of initial regression parameters is greatly expedited by use of a graphical procedure adapted from Ref. 5. Assuming for the moment that the PSDF can be represented by a two-parameter, single mode basis function (we have used expeditious computer approximations to zeroth order lognormal basis functions and Gaussian basis functions), one can plot the contours of constant residual error (\sqrt{Q} expressed as percent) versus the two regression parameters. The minima of such a plot suggest approximate values for the modal diameter and width of each mode of the PSDF. Further, one can immediately see which limits should be chosen for the minimum and maximum diameters of the inversion. This feature is quite significant for the constrained eigenfunction technique, but less important for the nonlinear regression technique.

The use of error contour plots does not assure a unique choice of regression parameters, given a stated imprecision level for the scattering inputs. It does suggest, however, which parameter sets are more likely to represent a correct inversion of the scattering data and which sets are merely artifices of the scattering kernels. The discrimination between correct and incorrect parameter sets is made on the basis of the depth of the relative minima in the residual error surface, assuming that the input errors are normally distributed about zero.

The above described procedure is not conclusive, since the shape of the error surface depends, to some extent, on the choice of basis function used for the plot. In addition, we have found that the residual error associated with the PSDF obtained by the nonlinear regression method is always equal to or less than the minimum error contour for a single mode basis function, since the regression method can use multi-mode basis functions.

Although it should not be solely relied upon to determine the PSDF regression parameters, we have found that the residual error contour analysis is a valuable adjunct to both PSDF inversion procedures described in this report.

3.0 INVERSION OF THE PSDF FROM NOISY, SYNTHETIC MIE SCATTERING DATA

The two previously described inversion techniques are here applied to the recovery of the PSDF from computer simulated Mie scattering data containing stated levels of Gaussian distributed noise. Since we have previously presented many recovered PSDF's (Ref. 1), we shall here be concerned with three specific situations: (1) multiwavelength scattering from nearly transparent droplets at a single scattering angle slightly less than the "rainbow angle" for the droplets; (2) multiwavelength backscattering (180 deg) from transparent particles; and (3) multiangle, single wavelength forward scattering from absorptive particles (carbon spheres).

The first situation illustrates the difficulty encountered when the kernels introduce artifices into the regression procedure. Figure 1 shows an assumed particle size distribution for a spray of n-butanol droplets, whose refractive indices are stated in Ref. 6. Figure 2 shows the set of spectral inputs (normalized by the mean of all inputs) which corresponds to the scattering of unpolarized light by these droplets into a spectrometer located at 135 deg scattering angle. The spectrometer's collection optics are assumed to subtend an angle of 6 deg for these calculations. Residual error contours for the recovery of the PSDF of Fig. 1 from the scattering spectrum of Fig. 2 are shown for the cases of zero and 6.7-percent input noise levels in Figs. 3 and 4, respectively. The recovered number normalized and mass normalized PSDF's for 10 sets of error-laden inputs (6.7-percent noise level) are shown in Figs. 5 and 6, respectively.

Figures 3 - 6 show that, in addition to the correct mode at $0.34 \mu\text{m}$ (with full width at half maximum (FWHM) of $0.25 \mu\text{m}$), the properties of this set of scattering kernels introduce false modes at other modal diameters. Particularly apparent is the erroneous mode near $1.2 \mu\text{m}$.

Significantly, the scattering inputs corresponding to single mode PSDF's at modal diameters of $0.34 \mu\text{m}$ and $1.2 \mu\text{m}$, a bimodal PSDF with modes at $1.06 \mu\text{m}$ and $1.3 \mu\text{m}$, and a trimode with modes at $0.34 \mu\text{m}$, $1.06 \mu\text{m}$, and $1.3 \mu\text{m}$ are almost indistinguishable from the scattering spectrum of Fig. 1. In fact, avoiding nonuniqueness in inverting PSDF's in the stated size range for this geometry requires experimental accuracy better than 2.3 percent. Attempts to deconvolve these PSDF's using the constrained eigenfunction expansion method with 12 optimally chosen wavelengths from the original set of 18 wavelengths were

totally unsuccessful, yielding modes near each of the four modal diameters suggested by Figs. 3 and 4, regardless of whether the scattering inputs corresponded to single mode, bimodal, or trimodal PSDF's in the size range shown.

This situation arose in an actual Mie scattering experiment recently carried out at the AEDC. The experiment was intended to obtain visible scattering data at 135 deg and infrared scattering data at 180 deg. The complete failure of the infrared portion of the experiment effectively prevented the PSDF from being recoverable for particles with diameters greater than $2 \mu\text{m}$ in the presence of an overwhelming number of small droplets. In addition, the previously described nonuniqueness in obtaining the PSDF for small particles was attributable to the lack of the infrared scattering channel.

Situation 2 involves simulated scattering by small latex spheres suspended in water using the refractive indices stated in Table 1. Since the absorption coefficients for latices are unknown at infrared wavelengths, the corresponding values in Table 2 are fictitious and are used here merely to complete the set of available scattering inputs. Simulated scattering data were generated for these wavelengths at 180-deg scattering angle (zero subtended angle) for the three PSDF's shown in Figs. 7, 11, and 15. The error free scattering inputs for these cases are listed in Tables 2-4. The number normalized PSDF's recovered from these inputs with 10 sets of noise added at 3-percent level are shown in Figs. 8, 12, and 16, respectively. Residual error contours for a single set of noisy inputs are shown for each case in Figs. 9, 13, and 17, respectively. Mass normalized recovered PSDF's are shown in Figs. 10, 14, and 18.

The number normalized PSDF shown in Fig. 11 strongly resembles a Junge power law distribution. It is, however, a truncated Gaussian distribution, centered on zero size. Note that the error contour plot in Fig. 13 exhibits a deep minimum near zero modal diameter, conforming fairly well to the recovered number normalized PSDF's shown in Fig. 12. The difference between this distribution and a true Junge distribution becomes apparent only when the mass normalized recovered PSDF's shown in Fig. 14 are considered. Similarly, although the number normalized, PSDF's in Figs. 15 and 16 are clearly bimodal, the equivalent mass normalized PSDF's in Fig. 18 are almost unimodal.

Efforts to deconvolve the scattering data of situation 2 using the constrained eigenfunction expansion were unsuccessful because of the lack of sufficient information content in the 180-deg backscattering kernels at the wavelengths of Table 1. Successful results were obtained when phase functions (ratios of differential scattering cross sections to extinction cross sections) were substituted for differential cross sections in both the scattering kernels and the simulated scattering inputs (integrated over the assumed PSDF). Backscattering phase functions have much more information at small particle sizes (below about $2.0 \mu\text{m}$) than do back scattering cross sections; consequently, nonlinear regressions obtained

using phase functions were also considerably more accurate than those which were based on backscattering cross sections. Unfortunately, these observations are only of academic interest, since in any practical experiment the light scattering signal is proportional to a suitably defined, scattering cross section. Consequently, the inversion kernels chosen for use in Eq. (1) must also be proportional to scattering cross sections, not to ratios of cross sections.

The third situation considered here is that of scattering at small forward angles by very absorptive aerosols (carbon). Because of the dipolar surface plasmon resonance (which occurs for carbon spheres at about $0.22 \mu\text{m}$ wavelength), carbon is very strongly absorptive at all wavelengths from the ultraviolet to the infrared. Consequently, little is gained by using additional wavelengths for particle size inversion experiments. The work of Ref. 1 suggests that the optimal scattering configuration for carbon aerosol size inversion experiments is a multiangular configuration whose smallest angle is about 5 deg (polarization information is lost at smaller angles) and whose wavelength is as small as the smallest particles of interest. Figure 19 shows the result of regression of the PSDF from ten sets of scattering inputs containing 5 percent noise level for a bimodal PSDF. The noise free inputs are stated in Table 5. Figure 20 shows the corresponding mass normalized PSDF's. The same scattering data have been deconvolved using the constrained eigenfunction expansion method. The recovered number normalized PSDF (corresponding to the average of 10 sets of noisy input data at 5 percent noise level) and the associated 68-percent confidence limits are shown in Fig. 21. Figure 22 shows the corresponding mass normalized PSDF. The constrained eigenfunction method yields good deconvolutions in this situation because the scattering kernels are much more sensitive to submicron particles than are those of the two previous situations. If success is to be assured using the constrained eigenfunction expansion method, it is imperative that the scattering inputs be optimally chosen for the size range spanned by the PSDF. In contrast, the choice of inputs is much less critical for the nonlinear regression method.

4.0 CONCLUDING REMARKS

This report has presented the characteristics of two particle size inversion methods: (1) a constrained eigenfunction expansion deconvolution technique, and (2) a nonlinear regression technique. Although both these methods were first presented in Ref. 1, the nonlinear regression method has not previously been described in the detail given in this report. In addition, the constrained eigenfunction expansion procedure has been improved by the incorporation of "active normalization" as described in Section 2.1.

The addition of this feature permits the constrained eigenfunction expansion deconvolution technique and the nonlinear regression technique to be compared on an equal footing. The results of that comparison are the following conclusions:

1. The nonlinear regression technique is more stable and less sensitive to choice of inputs than is the constrained eigenfunction expansion technique. In some scattering geometries, the nonlinear regression technique can recover a fairly accurate PSDF using kernels with insufficient information content for deconvolutions based on the constrained eigenfunction expansion technique. This conclusion was stated in Ref. 1, but, until the incorporation of "active normalization" in the constrained eigenfunction expansion method, it was uncertain whether the greater stability of the nonlinear regression technique was due to the use of "passive normalization" in the constrained eigenfunction expansion method. Although "active normalization" does improve the deconvolution in some respects, it does not, apparently, reduce the threshold of kernel information content required for successful recovery of the PSDF.
2. The nonlinear regression technique is less versatile than the constrained eigenfunction expansion technique. Currently, only bimodal PSDF complexity can be treated, using completely free parameters. A trimodal PSDF can be recovered by a multi step approach in which the three modal diameters are frozen at the values suggested by the residual error contour analysis described in Section 2.3. The widths and relative heights of these three modes are then treated as free parameters. This approach permits the regression to be reduced in scope from eight free parameters to five free parameters. The latter is the same as the number of free parameters required for regression of a bimode. In contrast, the use of twelve scattering inputs in the constrained eigenfunction expansion deconvolutions is equivalent to regression of a tetramodal PSDF. In general $3N-1$ free parameters are required by either procedure to recover a PSDF whose complexity is represented by N modes.
3. The nonlinear regression method currently runs on a large mainframe computer. In contrast, the constrained eigenfunction expansion method can be run on minicomputers and microcomputers. Although some reduction in program complexity is anticipated, it is unlikely that a small computer version of the nonlinear regression algorithm described in this report will be developed for recovery of PSDF's with greater than single mode complexity. Thus, future Mie scattering-based particle sizing instrument package development must either include provision for remote terminal access to a mainframe computer or else incorporate into an onboard small computer PSDF inversion algorithms whose computational requirements are less demanding than the nonlinear regression technique. If the latter choice is made it must, of necessity, be made with the full recognition that the determination of a nearly optimal scattering geometry is a corollary requirement for the design of a self-contained particle sizing system.

REFERENCES

1. Curry, B. P. and Kiech, E. L. "Two Particle Size Inversion Procedures for Interpretation of Mie Scattering Measurements." AEDC-TR-83-32, in publication.
2. Curry, B. P. , Vorhees, L. C., and Kiech, E. L. "Development of Computer Codes to Invert the Particle Size Distribution Function of Homogeneous Spherical Aerosols from Mie Scattering Measurements." AEDC-TR-82-11 (AD-B069616), November 1982.
3. Capps, C. D., Henning, R. L., and Hess, G. M. "Analytic Inversion of Remote Sensing Data." *Applied Optics*, Vol. 21, No. 19, 1 October 1982, pp. 3581-3587.
4. Twomey, S. "The Application of Numerical Filtering to the Solution of Integral Equations Encountered in Indirect Sensing Measurement." *Journal of the Franklin Institute*, Vol. 279, No. 2, February 1965, pp. 95-189.
5. Kerker, M. *The Scattering of Light and Other Electromagnetic Radiation*. Academic Press, New York, 1969.
6. Sethna, P. P. and Williams, D. "Optical Constants of Alcohols in the Infrared." *Journal of Physical Chemistry*, Vol. 83, No. 3, February 1979, pp. 405-409.

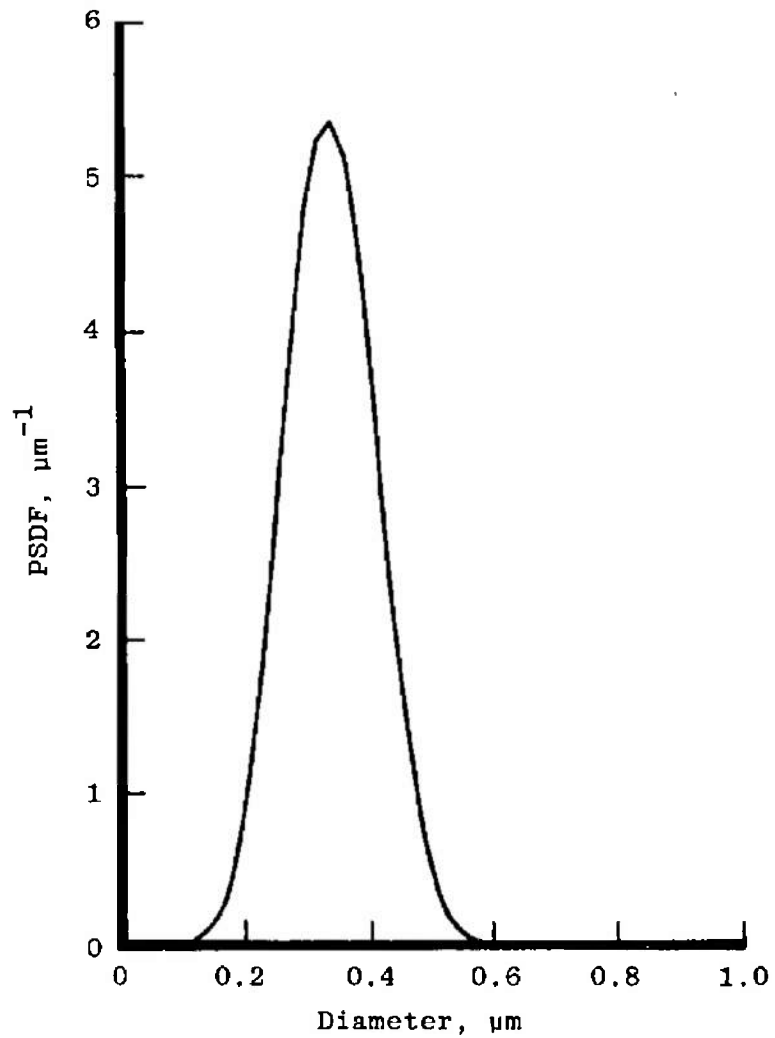


Figure 1. Number normalized particle size distribution function used to generate the scattering input spectrum of Fig. 2.

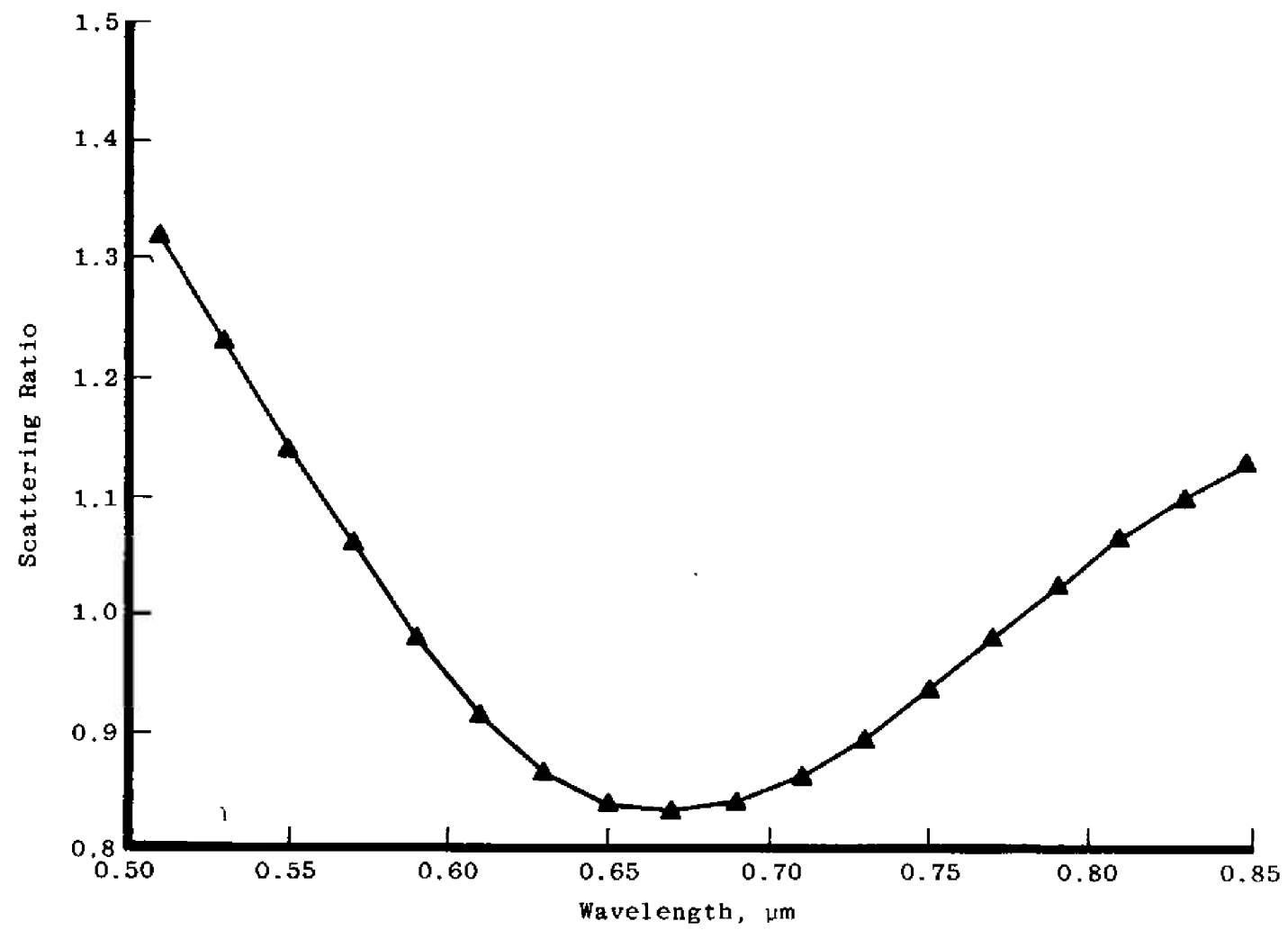


Figure 2. Computed backscattering spectrum for n-butanol droplets having the PSDF shown in Fig. 1.

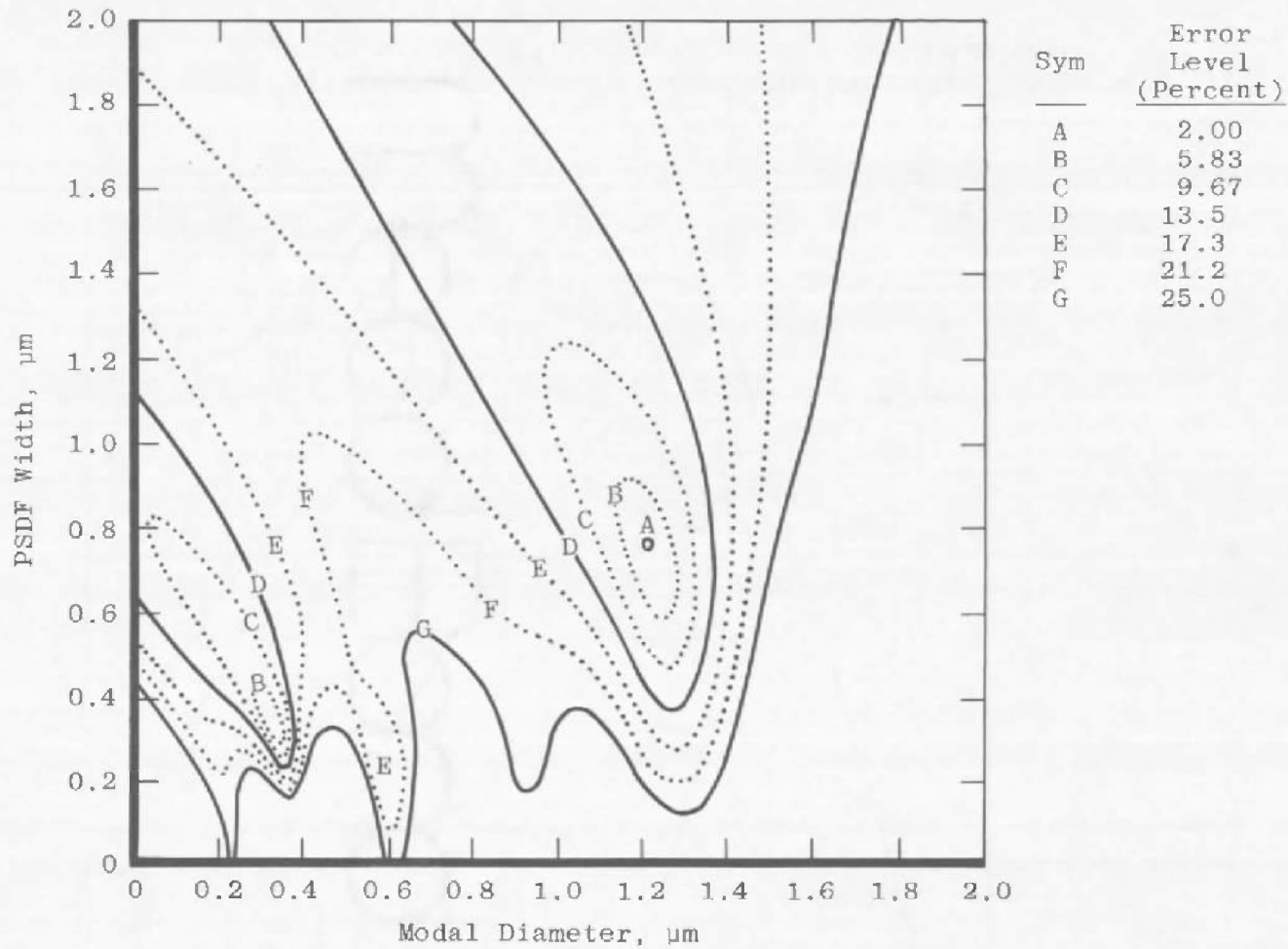


Figure 3. Residual error contours for recovery of the PSDF of Fig. 2 from the scattering inputs of Fig. 1 - no additional noise.

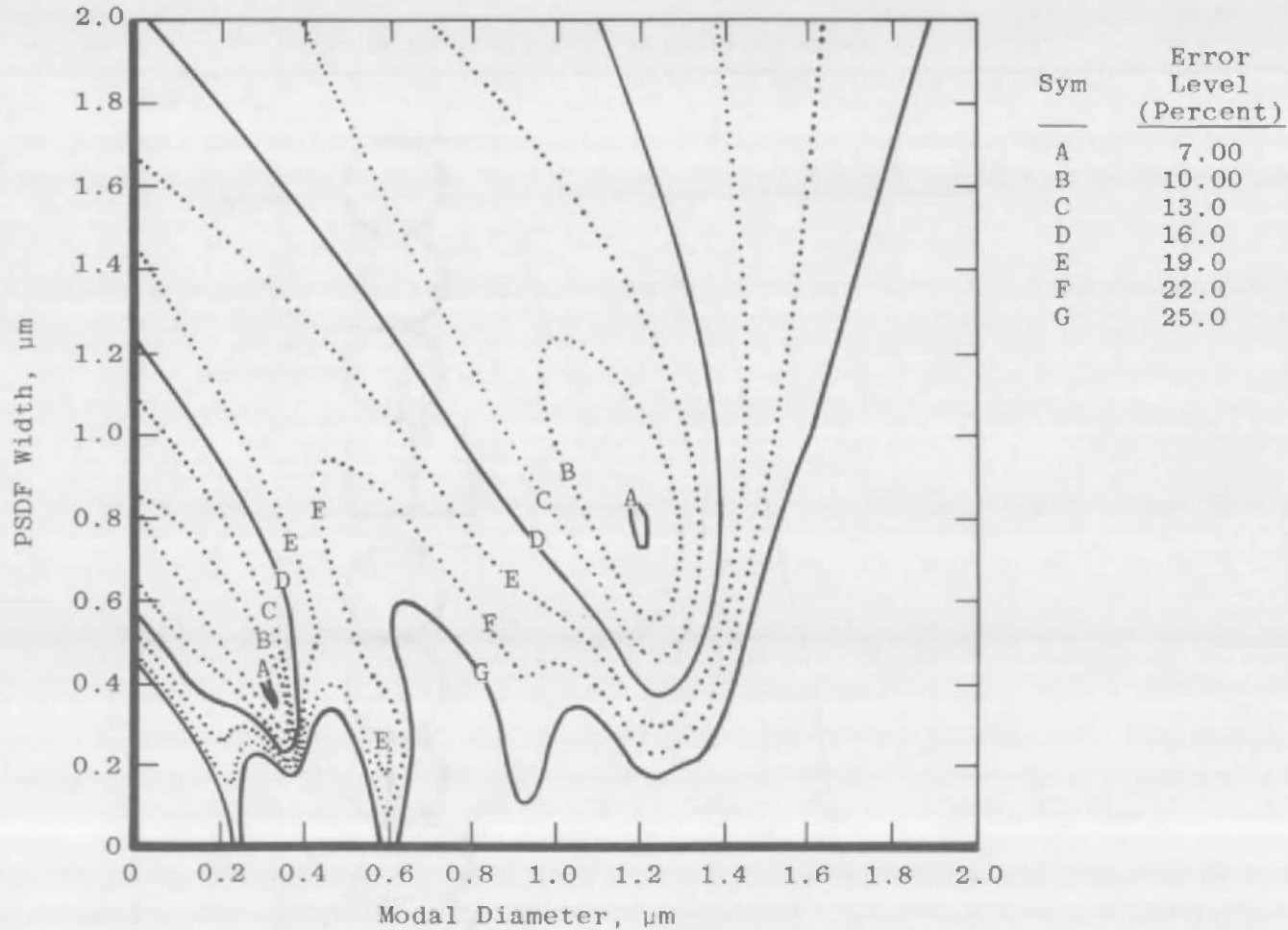


Figure 4. Residual error contours for recovery of the PSDF of Fig. 2 from the scattering inputs of Fig. 1 with 6.7-percent Gaussian noise level.

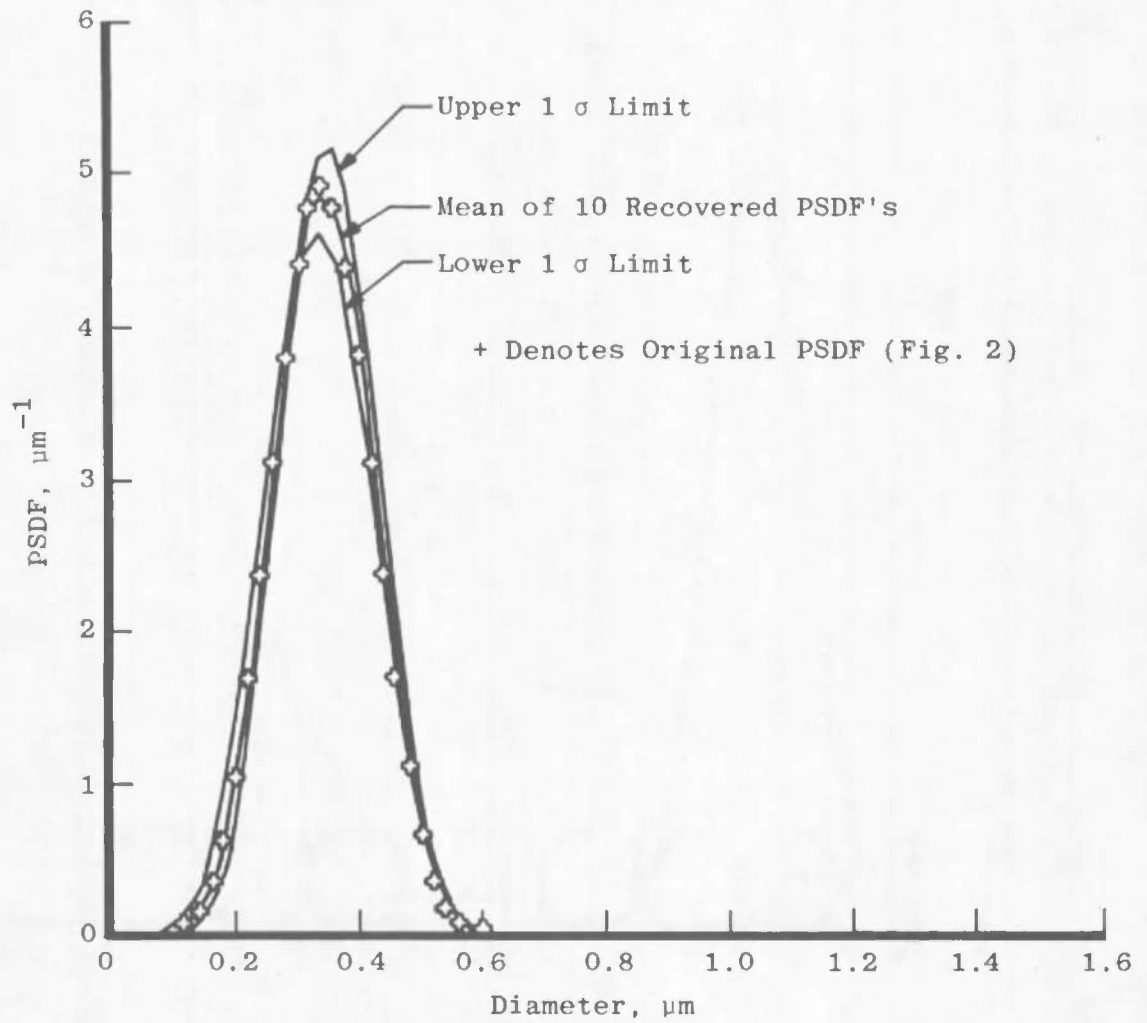


Figure 5. Number normalized PSDF recovered from the scattering inputs of Fig. 1 with 6.7-percent Gaussian noise level.

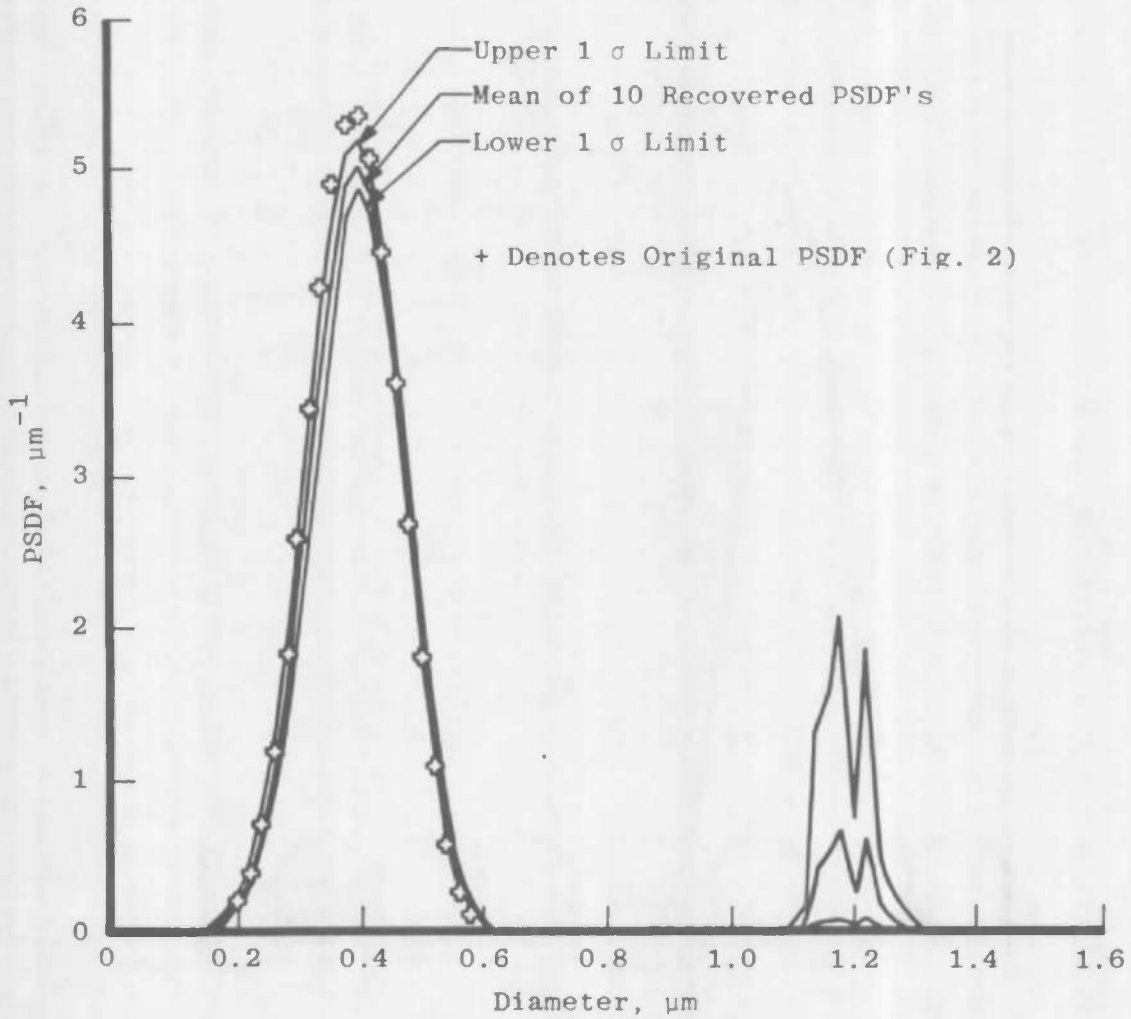


Figure 6. Mass normalized PSDF recovered from the scattering inputs of Fig. 1 with 6.7-percent Gaussian noise level.

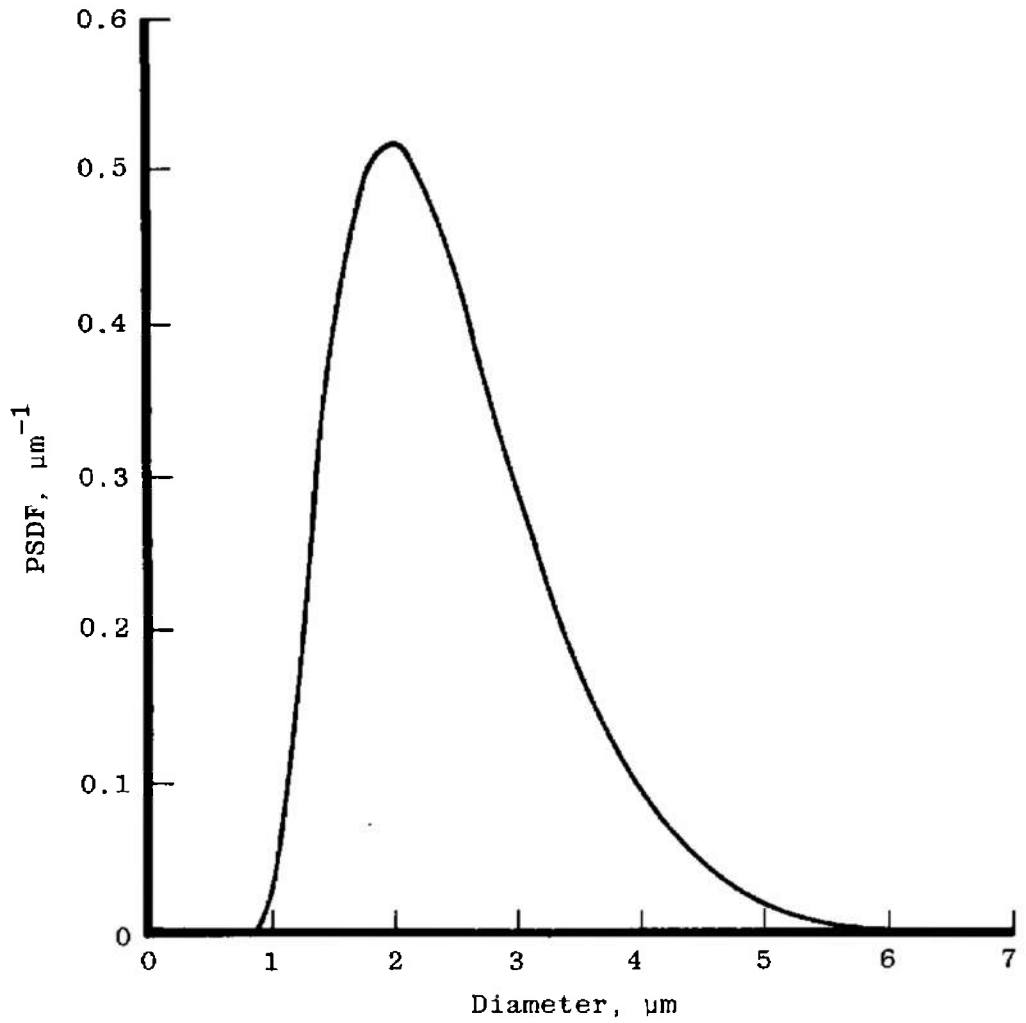


Figure 7. Number normalized PSDF used to generate the scattering inputs in Table 2.

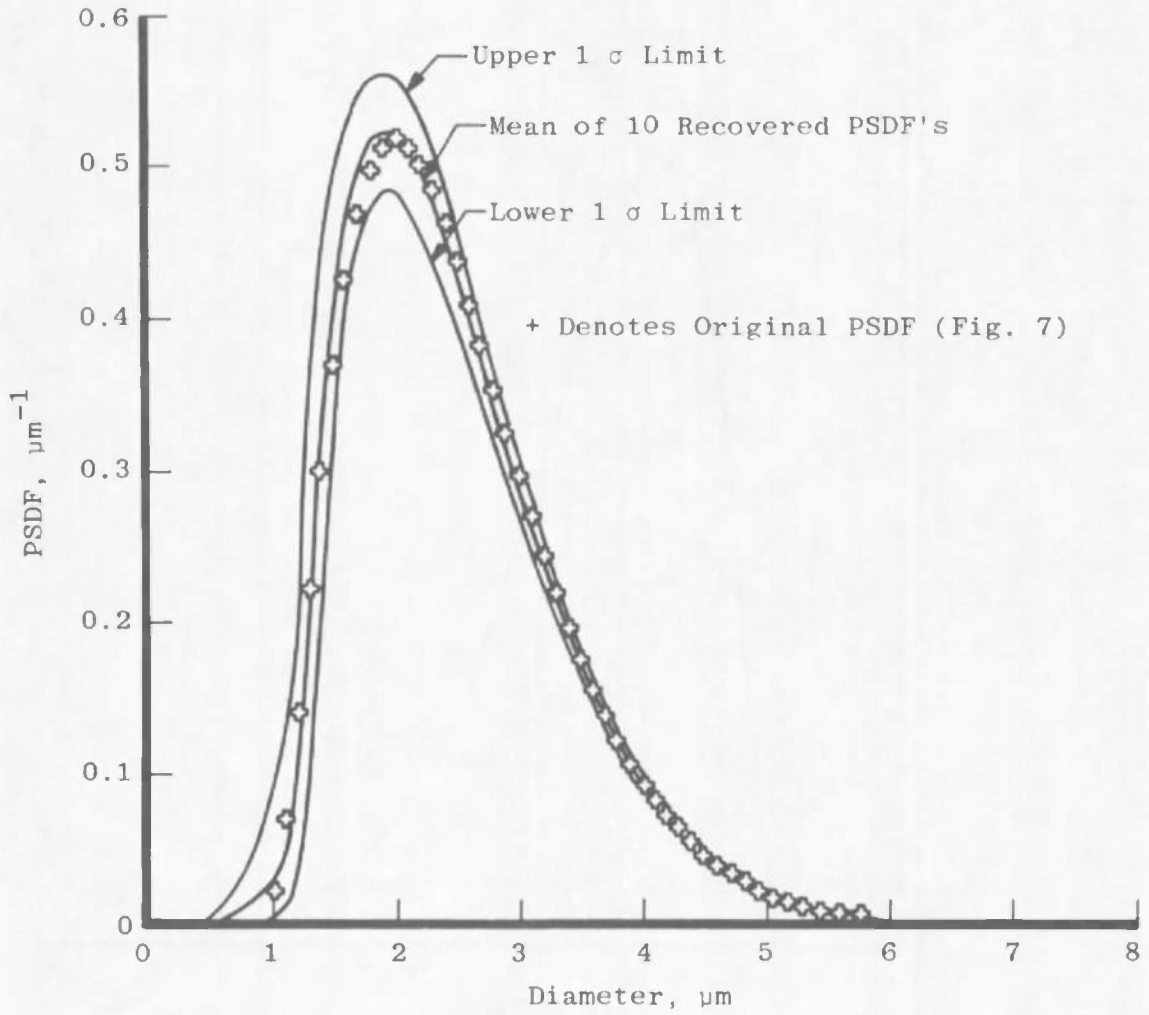


Figure 8. Number normalized PSDF recovered from the scattering inputs of Table 2 with 3-percent Gaussian noise level.

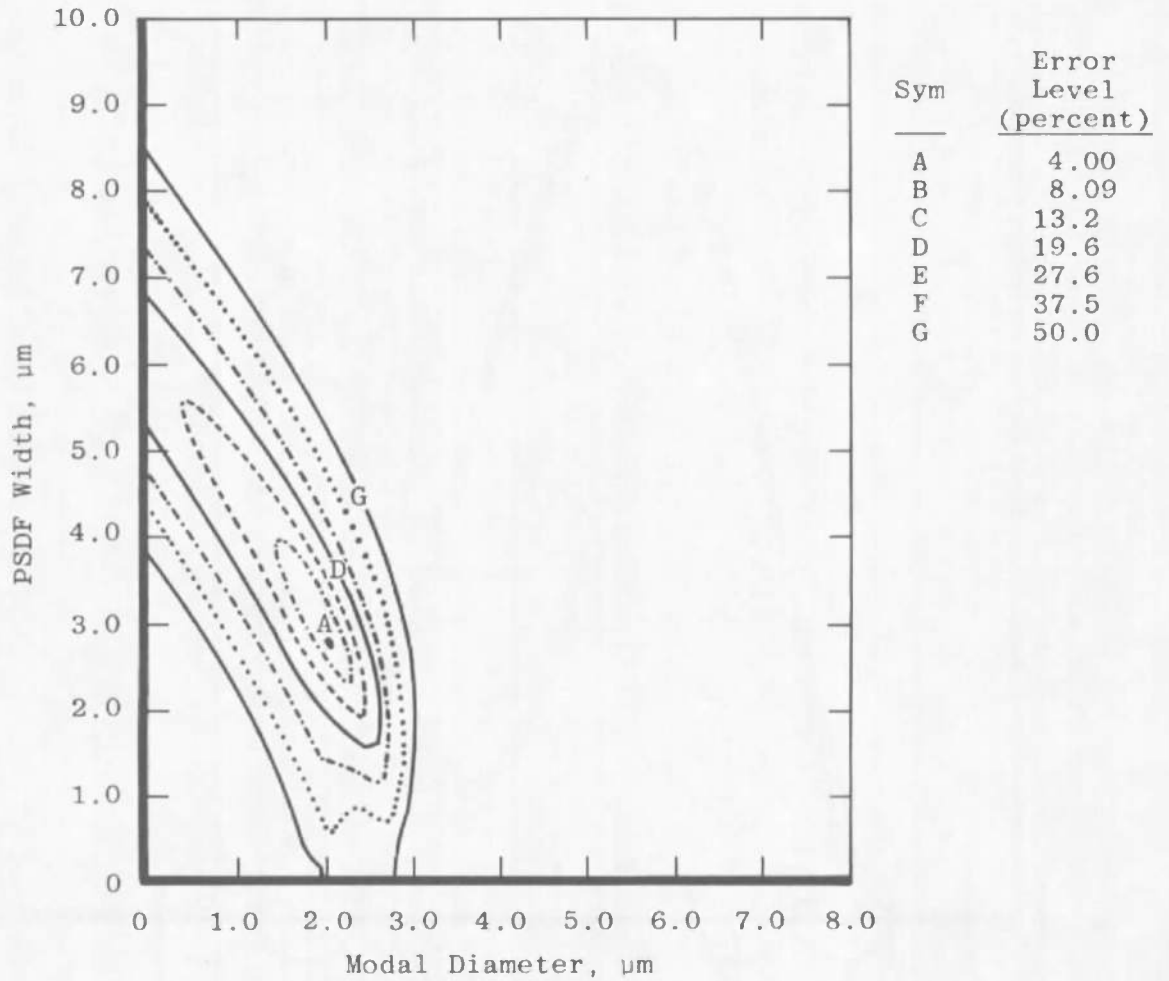


Figure 9. Residual error contours for recovery of the PSDF of Fig. 7 from the scattering inputs listed in Table 2.

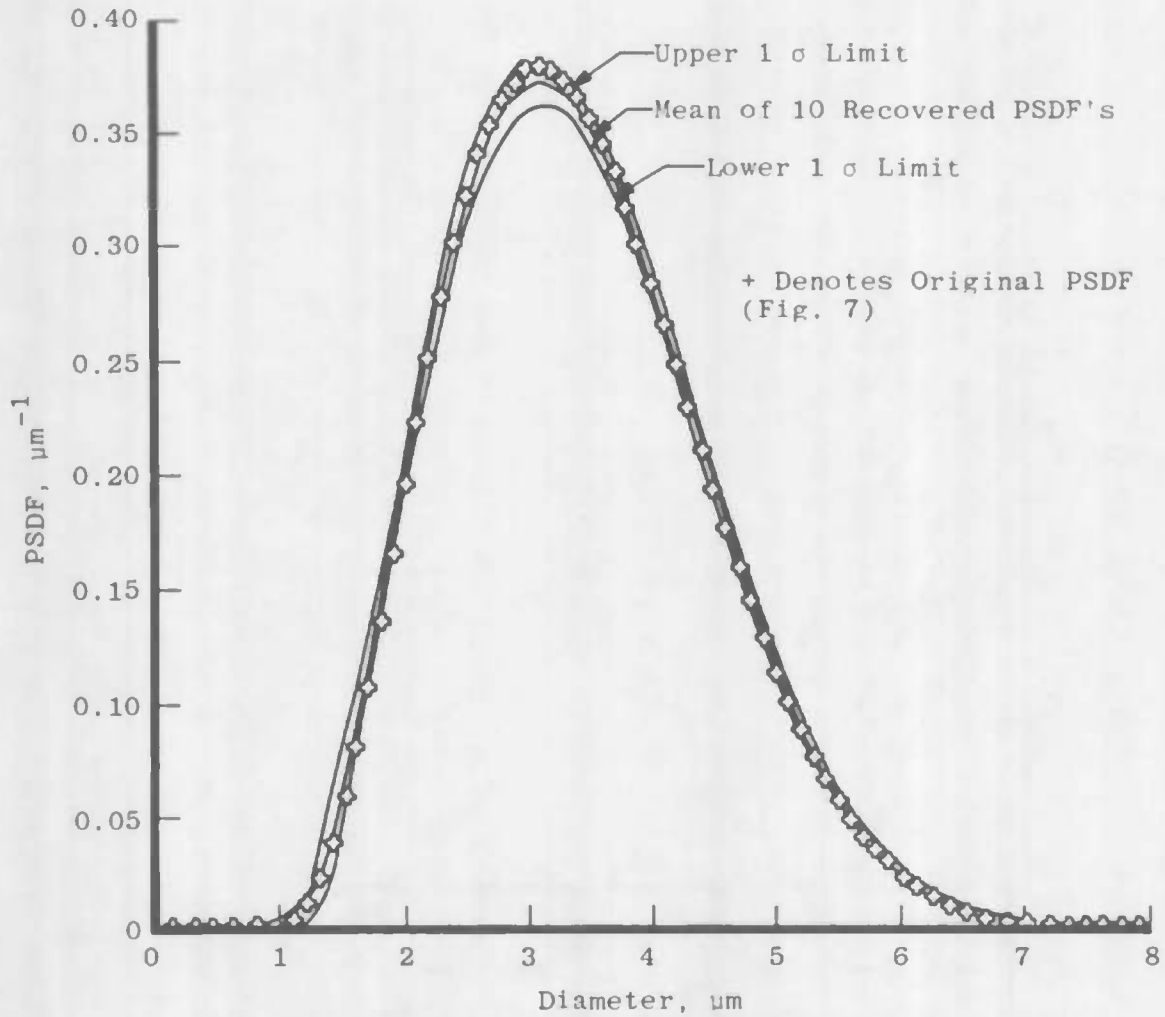


Figure 10. Mass normalized PSDF recovered from the scattering inputs of Table 2 with 3-percent Gaussian noise level.

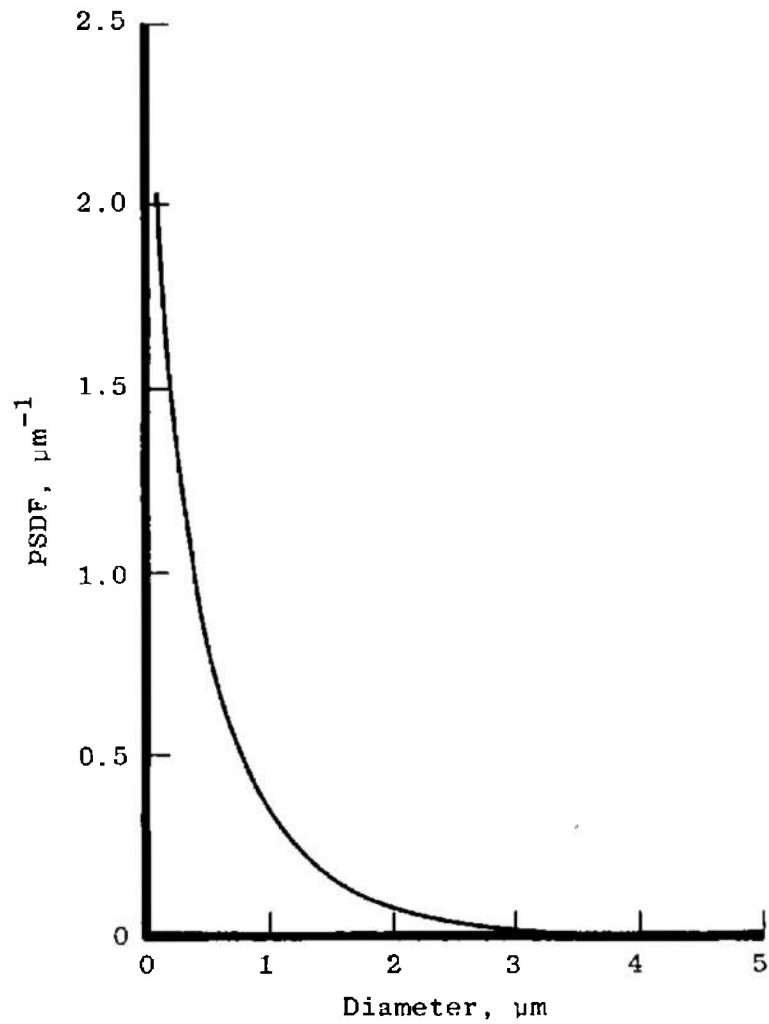


Figure 11. Number normalized "zero centered" PSDF used to generate the scattering inputs in Table 3.

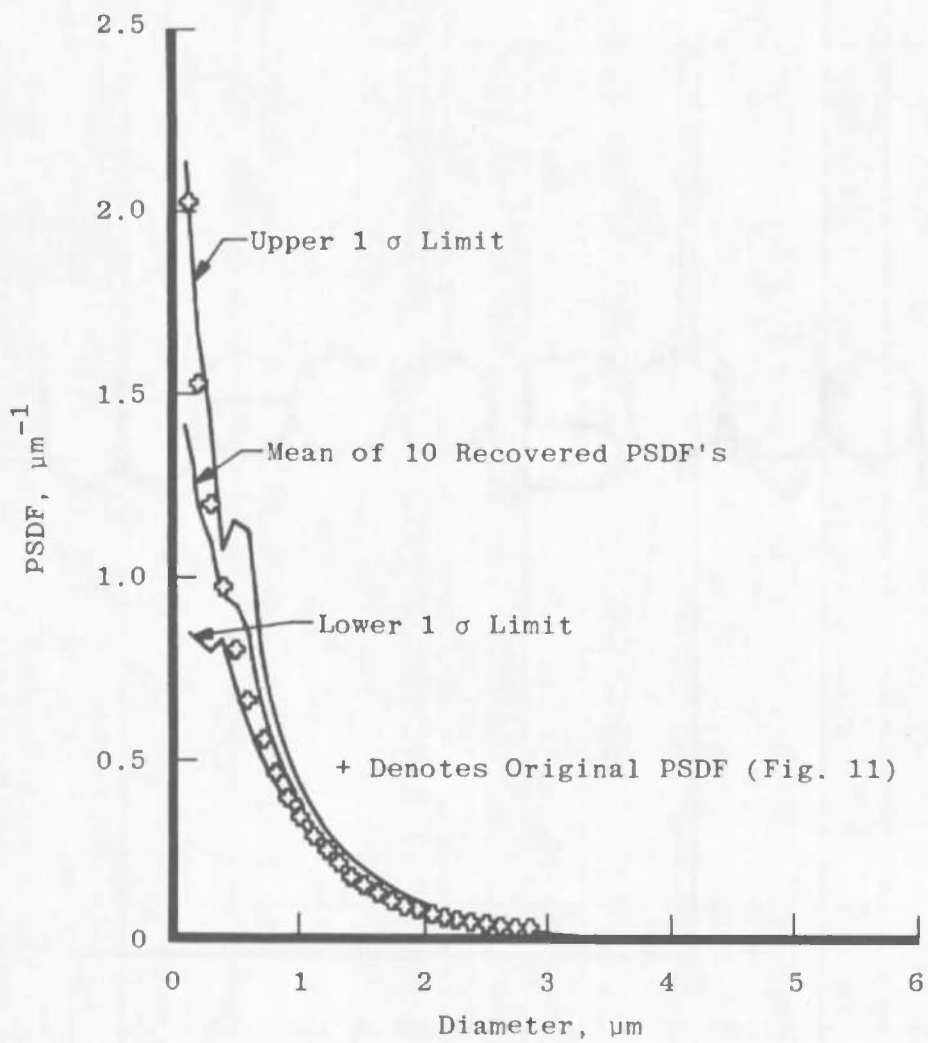


Figure 12. Number normalized PSDF recovered from the scattering inputs of Table 3 with 3-percent Gaussian noise level.

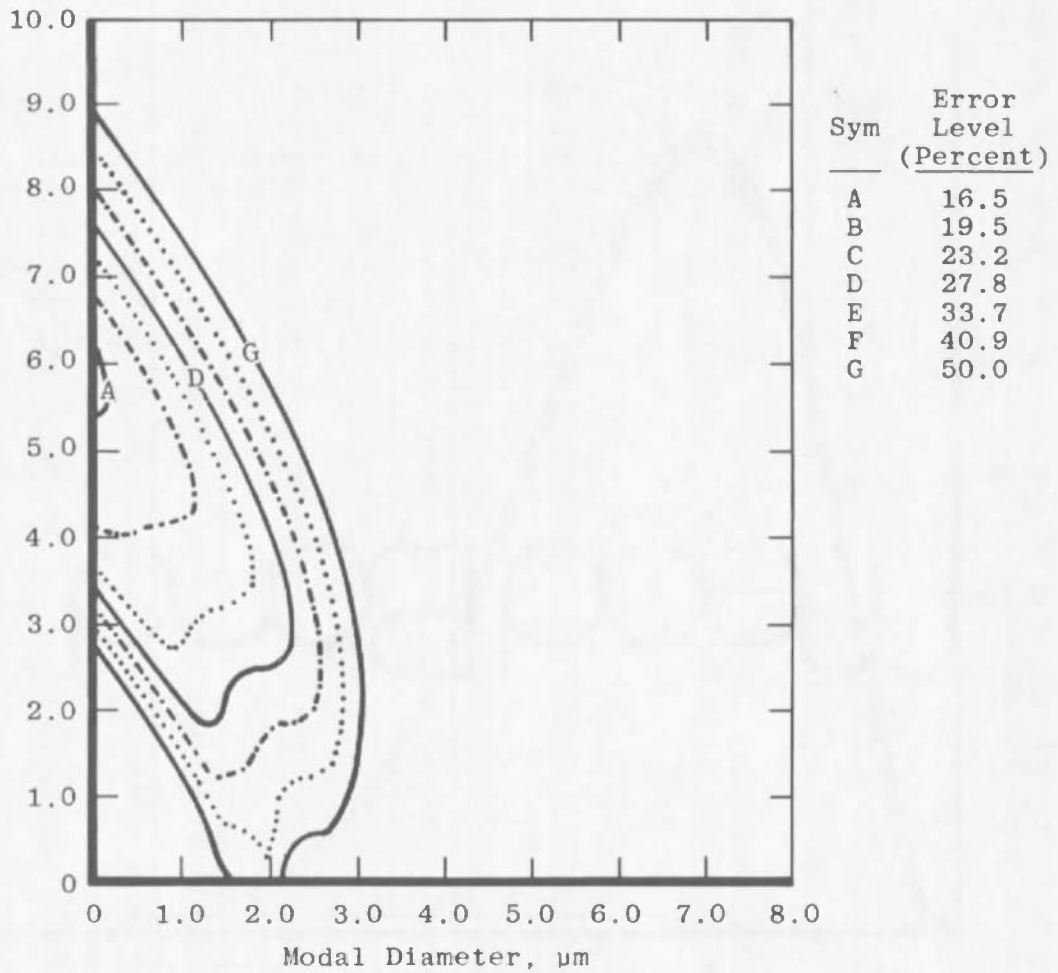


Figure 13. Residual error contours for recovery of the PSDF of Fig. 11 from the scattering inputs listed in Table 3.

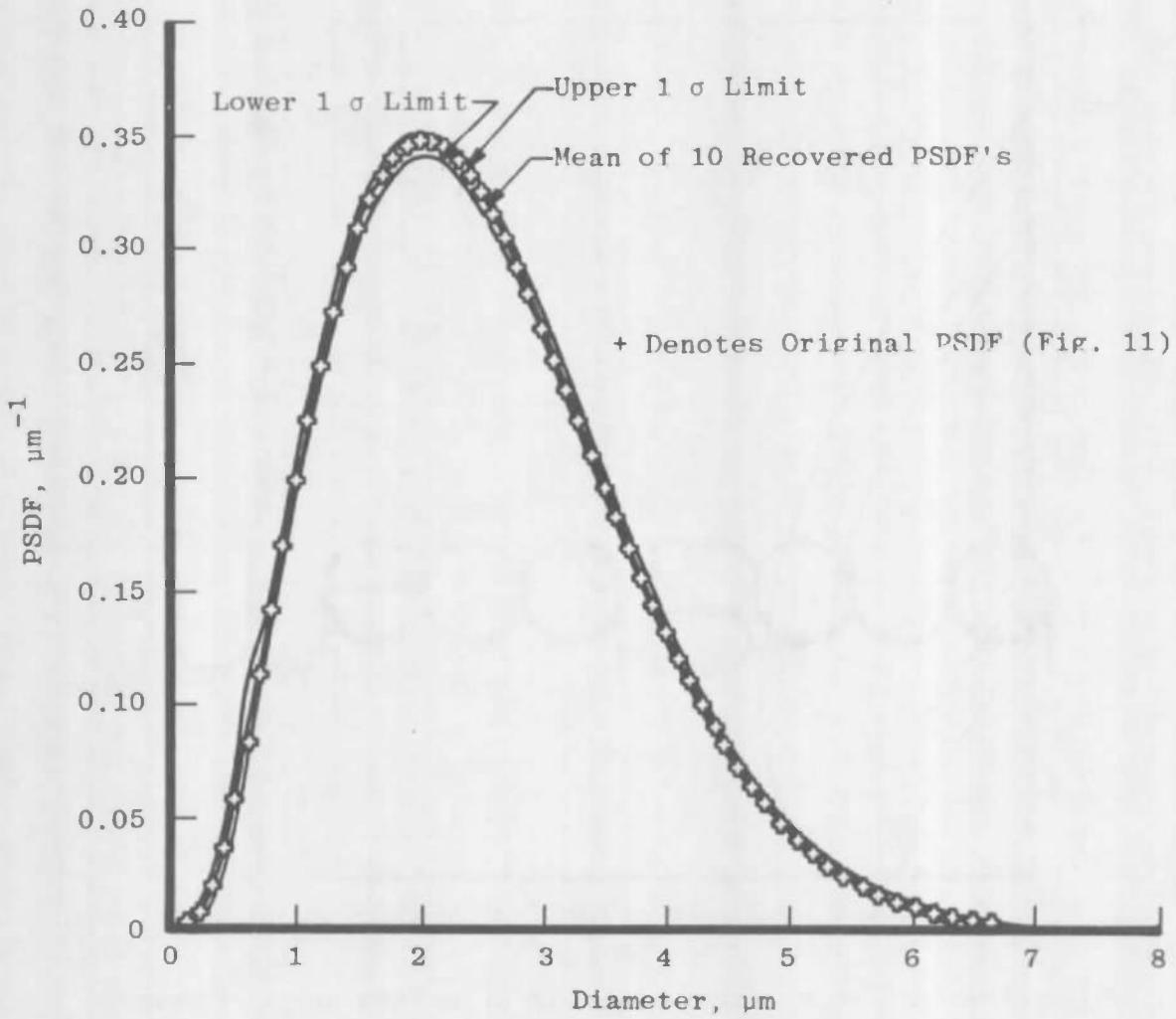


Figure 14. Mass normalized PSDF recovered from the scattering inputs of Table 3 with 3-percent Gaussian noise level.

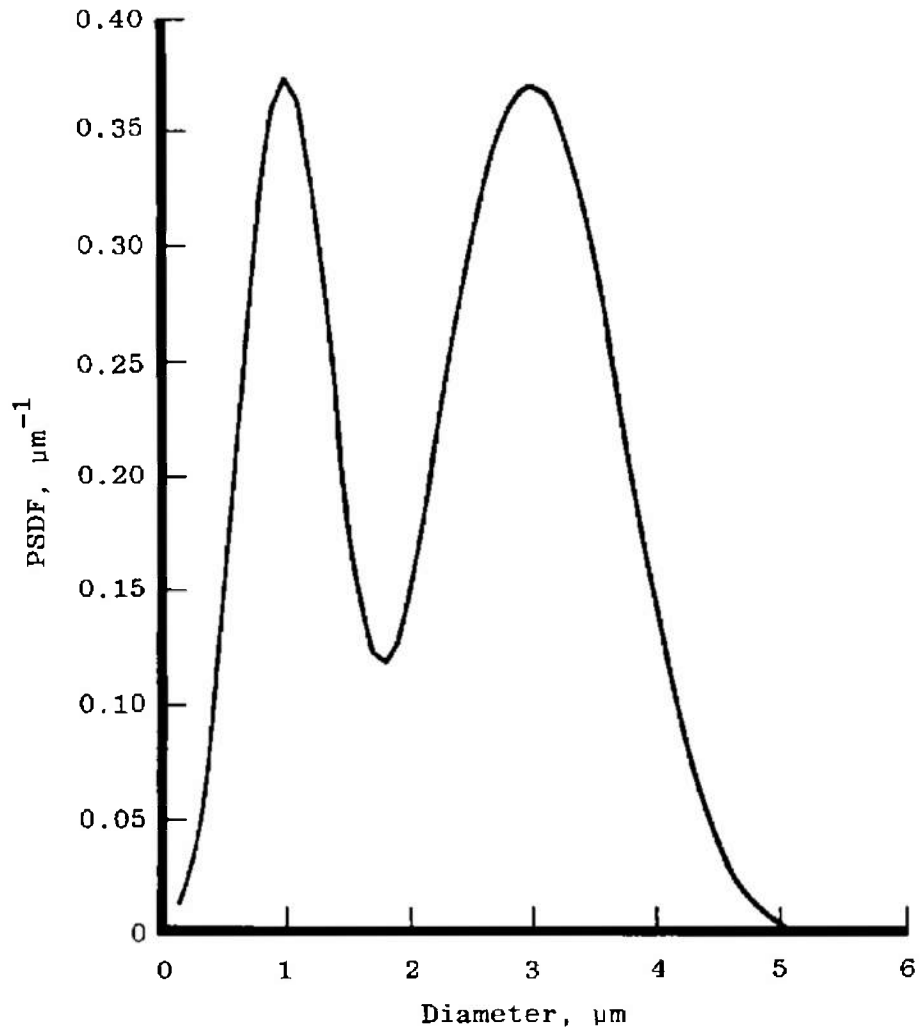


Figure 15. Number normalized bimodal PSDF used to generate the scattering inputs in Table 4.

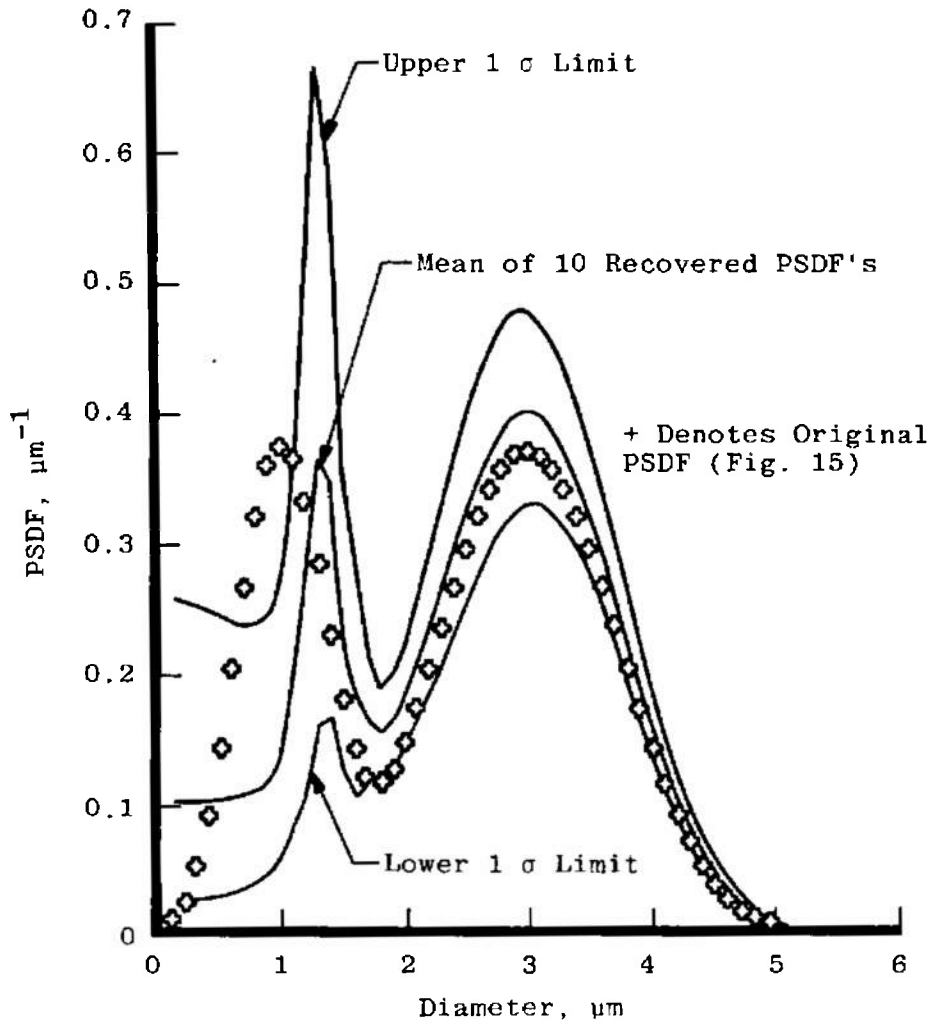


Figure 16. Number normalized PSDF recovered from the scattering inputs of Table 4 with 3-percent Gaussian noise level.

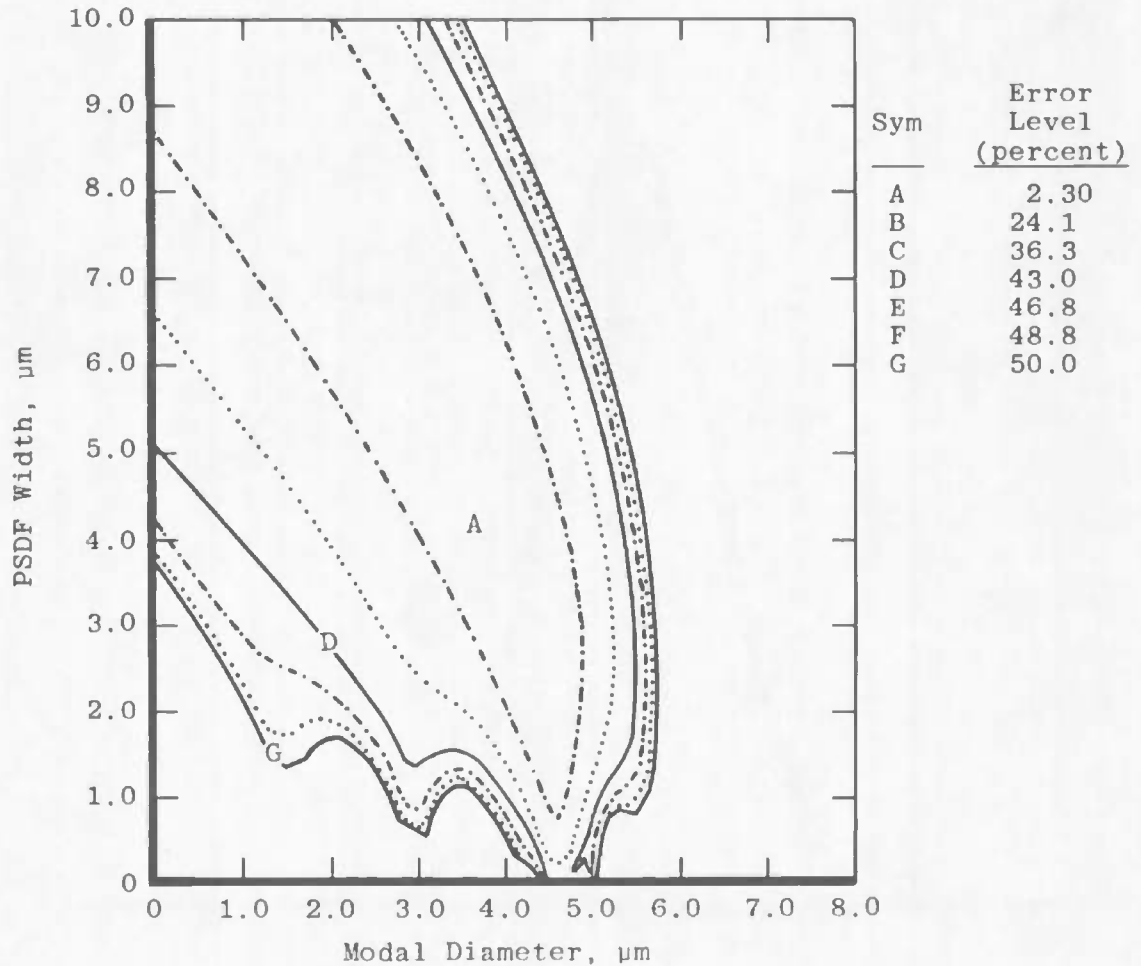


Figure 17. Residual error contours for recovery of the PSDF of Fig. 15 from the scattering inputs listed in Table 4.

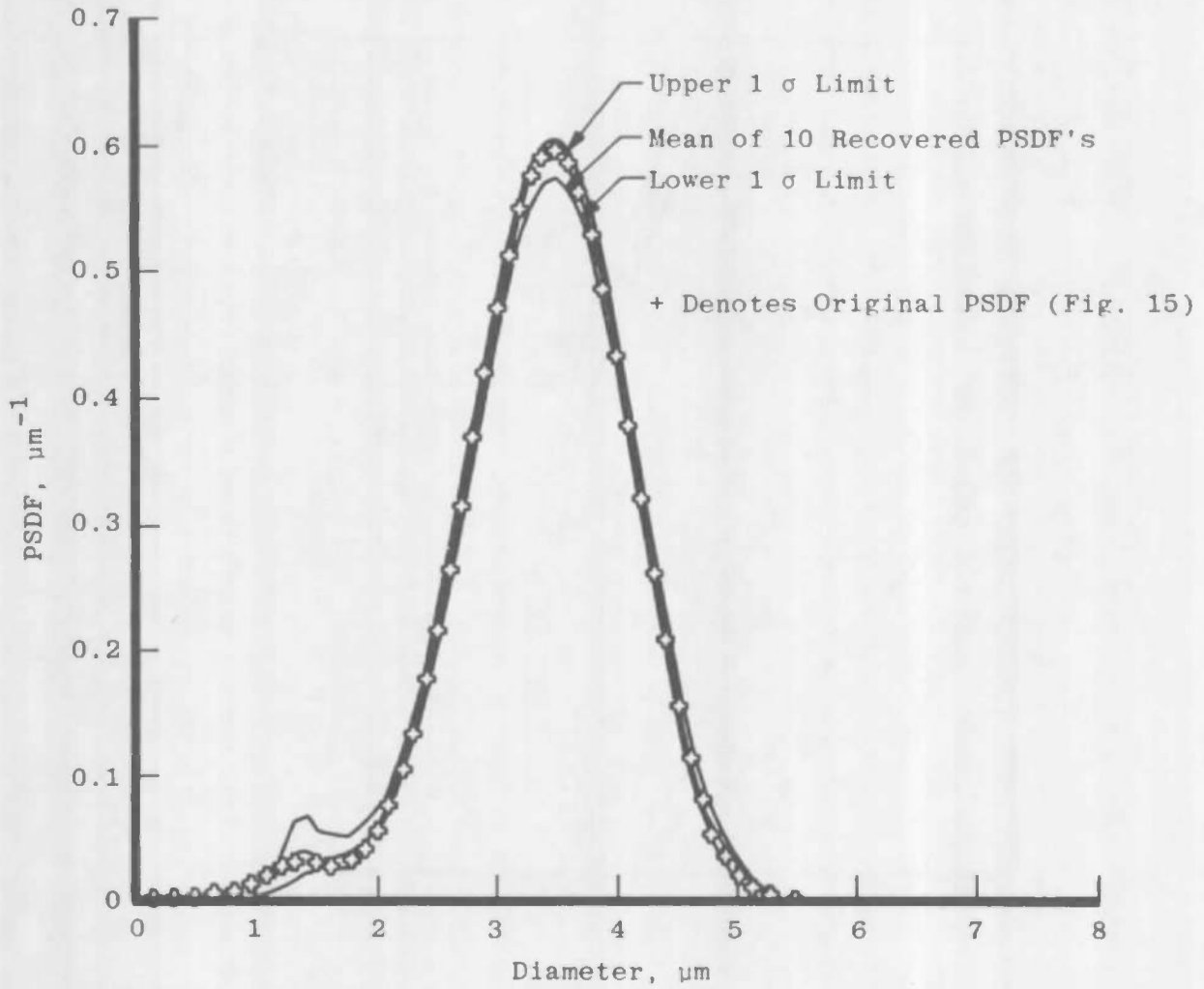


Figure 18. Mass normalized PSDF recovered from the scattering inputs of Table 4 with 3-percent Gaussian noise level.

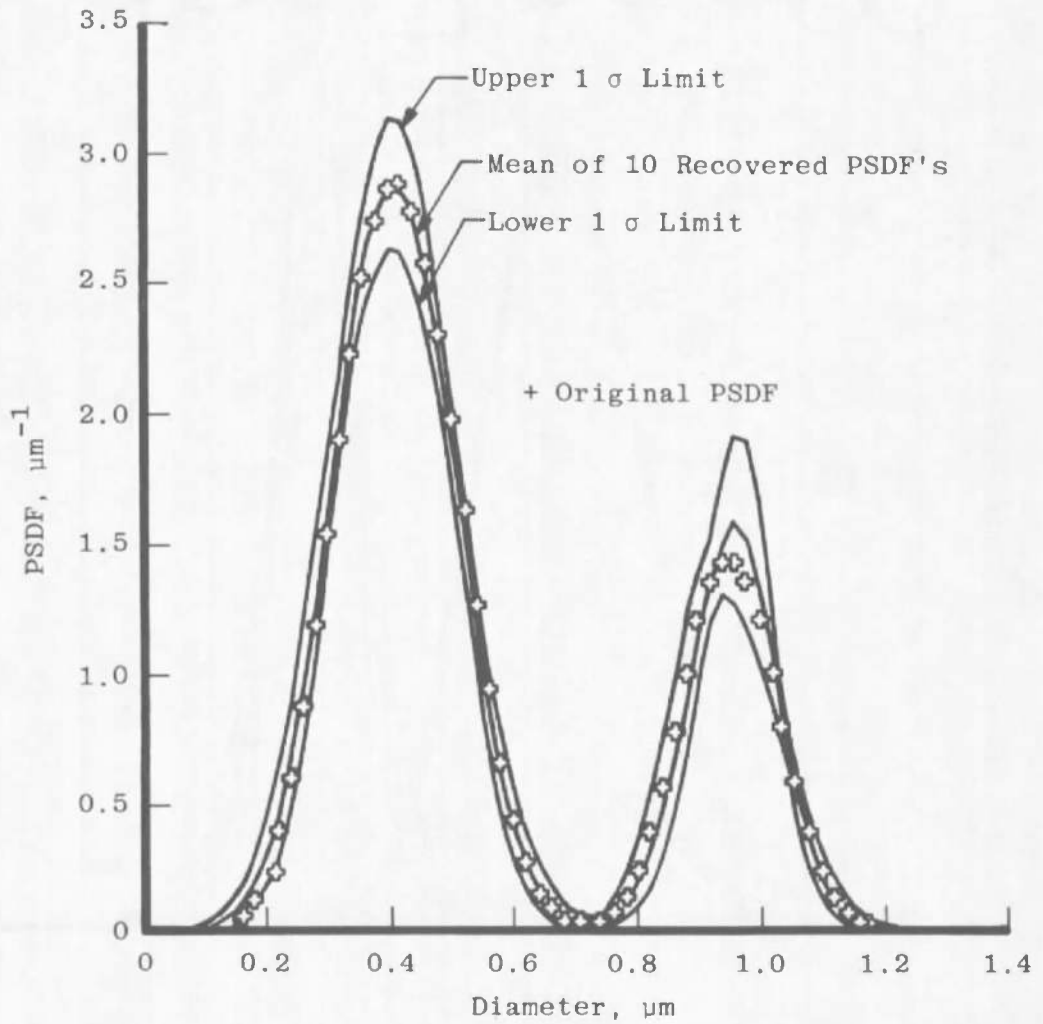


Figure 19. Number normalized bimodal PSDF regressed from the scattering inputs of Table 5 with 5-percent Gaussian noise level.

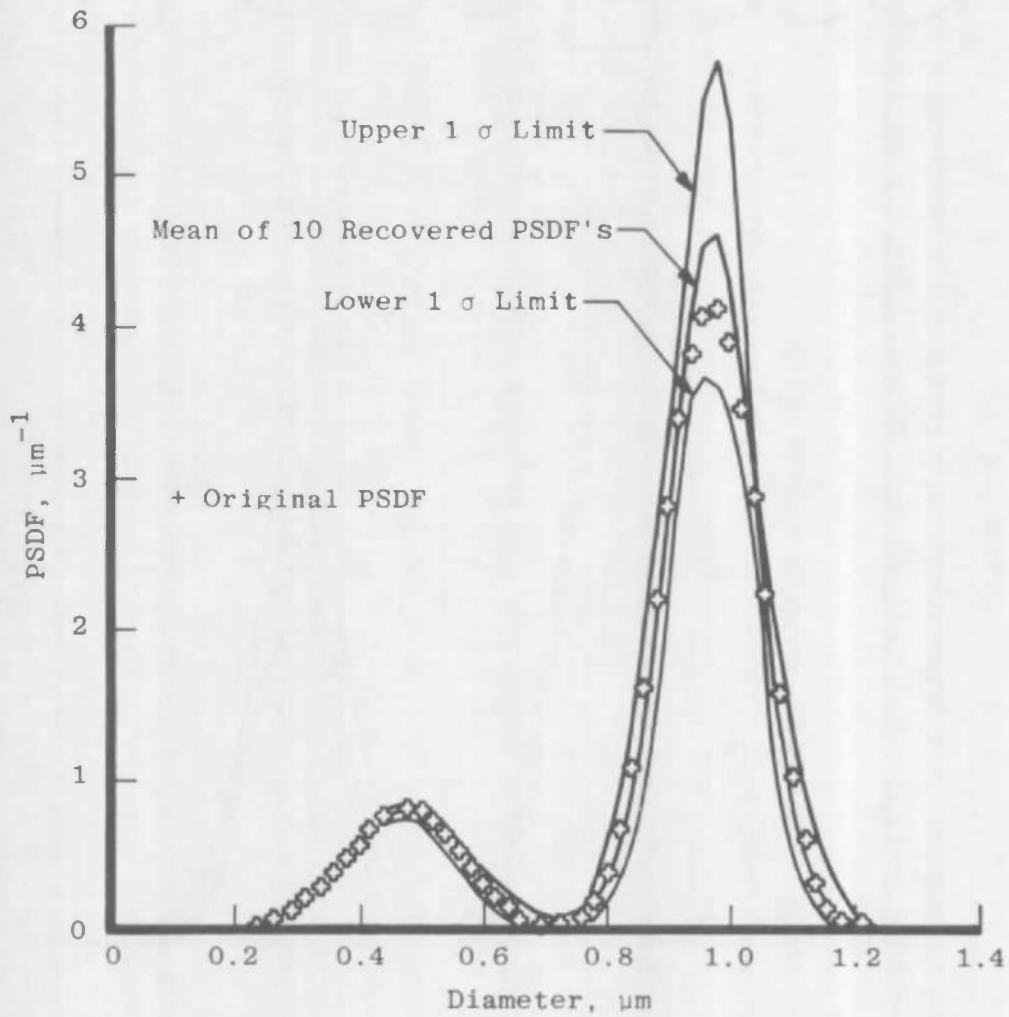


Figure 20. Mass normalized bimodal PSDF regressed from the scattering inputs of Table 5 with 5-percent Gaussian noise level.

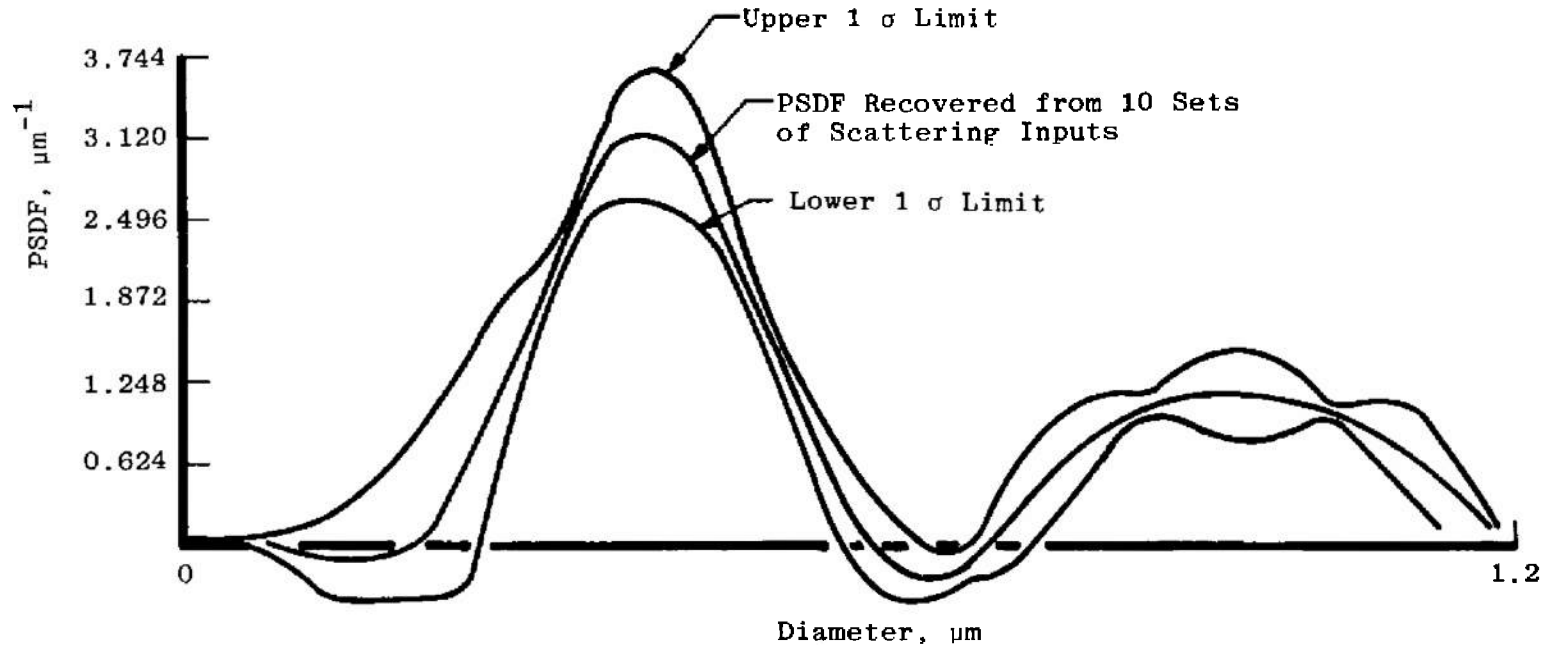


Figure 21. Number normalized bimodal PSDF deconvolved from the scattering inputs of Table 5 with 5-percent Gaussian noise level.

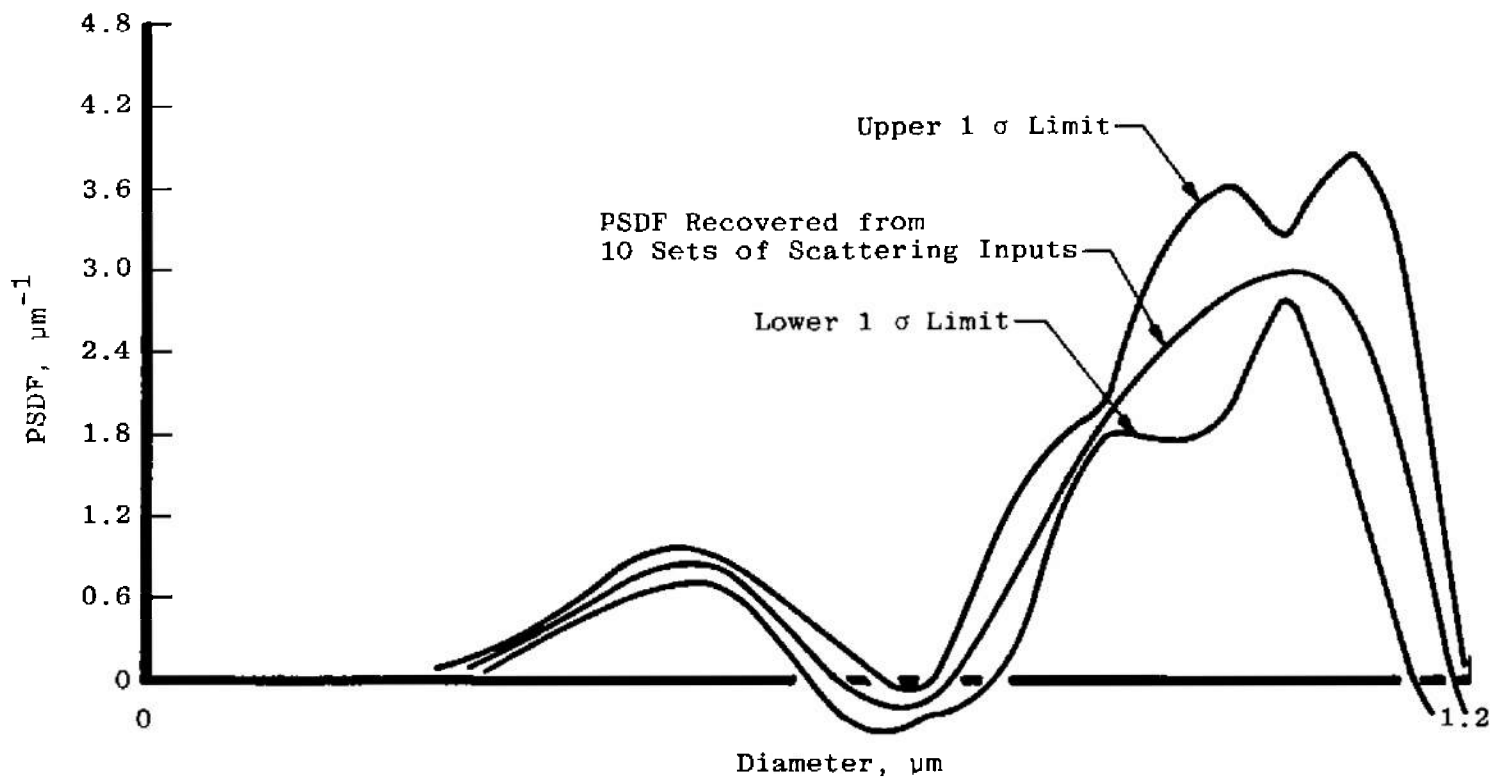


Figure 22. Mass normalized bimodal PSDF deconvolved from the scattering inputs of Table 5 with 5-percent Gaussian noise level.

Table 1. Refractive Indices used to Generate the Scattering Inputs Listed in Tables 2 - 4

Wavelength, μm	Refractive Index (real)
0.222	1.381
0.266	1.299
0.524	1.202
0.782	1.191
1.04	1.191
1.55	1.203
2.33	1.340
2.59	1.133
2.85	1.153
3.63	1.178
3.88	1.186
4.14	1.201
4.91	1.173
6.20	1.213
8.99	1.329

Table 2. Error-Free Scattering Inputs for the PSDF in Fig. 7

Wavelength, μm	Scattering Inputs*
0.222	4.85
0.266	5.89
0.524	1.60
0.782	0.426
1.04	2.28
1.55	0.172
2.33	0.969
2.59	0.0518
2.85	0.0761
3.63	0.100
3.88	0.107
4.14	0.122
4.91	0.075
6.20	0.109
8.99	0.223

*Normalized by the mean of all inputs.

Table 3. Error-Free Scattering Inputs for the PSDF in Fig. 11

Wavelength, μm	Scattering Inputs*
0.222	6.26
0.266	5.40
0.524	0.911
0.782	0.317
1.04	0.227
1.55	0.225
2.33	0.836
2.59	0.0615
2.85	0.0838
3.63	0.105
3.88	0.111
4.14	0.125
4.91	0.0835
6.20	0.103
8.99	0.154

*Normalized by the mean of all inputs.

Table 4. Error-Free Scattering Inputs for the PSDF in Fig. 15

Wavelength, μm	Scattering Ratio*
0.222	4.40
0.266	6.03
0.524	1.64
0.782	0.411
1.04	0.272
1.55	0.134
2.33	1.14
2.59	0.0597
2.85	0.0888
3.63	0.115
3.88	0.122
4.14	0.140
4.91	0.0711
6.20	0.0899
8.99	0.286

*Normalized by the mean of all inputs.

Table 5. Error-Free Scattering Inputs for the PSDF in Fig. 19

Angle, deg	Polarized Scattering Inputs*	
	Perpendicular	Parallel
5	3.19	2.96
10	1.64	1.17
15	0.713	0.520
20	0.625	0.335
25	0.305	0.128
30	0.271	0.141

*Normalized by the mean of all inputs.

NOMENCLATURE

a_i	Arbitrary expansion coefficients [see Eq. (15)]
C_i	Constrained solution PSDF linear expansion coefficient
C_i^o	Direct solution linear expansion coefficient
C_i^T	Trial PSDF linear expansion coefficient
D	Particle diameter
$E(y_i)$	Residual error associated with the "ith" scattering channel
$f(X)$	Number normalized particle size distribution function (PSDF)
$f^o(X)$	Error-free PSDF
$f^T(X)$	Trial PSDF
$G(y_i)$	Scattering input ratio associated with the "ith" scattering channel
$K(X, y_i)$	Scattering kernel associated with the "ith" scattering channel—[see Eq. (1)]
$K_o(X)$	Reference scattering kernel
$M(X, X)$	Symmetric kernel operator
N	Total number of scattering inputs
$N(y_i, y_j)$	Kernel covariance matrix element
N_o	Normalization function—[see Eq. (1)]
$U_i(y_k)$	Element of the "ith" eigenvector of the kernel covariance matrix
P_i	Nonlinear regression parameter
X	Particle size parameter

Y_i	Independent scattering variable (wavelength, angle, polarization, etc.)
γ	Smoothing parameter (Lagrange multiplier) used in the constrained eigenfunction expansion procedure
$\Delta f(X)$	Recovered PSDF uncertainty associated with stated input imprecision values
$\Delta G(y_i)$	Estimated imprecision associated with the "ith" scattering input ratio
$\delta G(y_i)$	Actual error in the "ith" scattering input ratio
$\phi_i(X)$	Eigenfunction of the symmetric kernel operator
λ	Incident light wavelength
λ_i	Eigenvalue of the kernel covariance matrix